

Signals of the electroweak phase transition at colliders and gravitational wave observatories

Mikael Chala,^a Claudius Krause,^b and Germano Nardini^c

^a*Institute of Particle Physics Phenomenology, Physics Department, Durham University, Durham DH1 3LE, UK*

^b*IFIC, Universitat de València-CSIC, Apt. Correus 22085, E-46071 València, Spain*

^c*Albert Einstein Center, Institute for Theoretical Physics, University of Bern, Sidlerstrasse 5, CH-3012 Bern, Switzerland*

E-mail: mikael.chala@durham.ac.uk, claudius.krause@ific.uv.es,
nardini@itp.unibe.ch

ABSTRACT: We explore new-physics setups that at low energy exhibit a Higgs potential with sizeable higher-dimensional operators. We focus on the parameter regions promoting a first-order electroweak phase transition (FOEWPT). For weakly-interacting setups, we find that such regions allowed by current data are always tuned when the operators receive contributions from integrating out $SU(2)_L$ singlets or triplets. The reason is the emergence of other operators that are naturally unavoidable and strongly experimentally constrained. The custodial quadruplet extension we propose, instead, does not suffer of this problem. We also analyse strongly interacting setups for which dimension-eight operators need to be considered. In this context we compute for the first time the parameters leading to a FOEWPT. We estimate the reach of LISA for probing all these low-energy scenarios and compare it with the capabilities of the Higgs measurements at current and future colliders. For some parameter regions, LISA can prove the existence of new physics before colliders.

KEYWORDS: Higgs physics, electroweak baryogenesis, phase transitions, gravitational waves, LHC, LISA

Contents

1	Introduction	1
2	A gap between the standard model and new physics	3
2.1	Thermal effects of \mathcal{O}_6 on the electroweak phase transition	4
2.2	Current LHC constraints	7
2.3	Concrete realizations	8
2.4	Phenomenology of quadruplets	11
2.4.1	The SM plus a $Y = 3/2$ quadruplet	11
2.4.2	A custodial quadruplet setup	12
2.5	Beyond the dimension-six effective field theory	14
3	The electroweak phase transition	16
3.1	Finite temperature potential	16
3.2	Mean-field estimates	18
3.3	Numerical procedure	20
4	Interplay between gravitational wave signatures and Higgs-self coupling measurements	23
4.1	The effect of other potentially relevant operators	24
5	Conclusions	27

1 Introduction

ElectroWeak (EW) baryogenesis [1] is an appealing setup to explain the matter-antimatter asymmetry of the Universe. For this to happen, the EW Symmetry Breaking (EWSB) must proceed via a Strong First Order EW Phase Transition (SFOEWPT). This is only possible if physics beyond the Standard Model (SM) exists, as such a transition requires the finite-temperature Higgs potential to behave radically differently from the one of the SM [2–5]¹.

Numerous extensions of the SM exhibiting a SFOEWPT have been considered in the literature. In most of the cases, the main ingredient to depart from the SM finite-temperature Higgs potential is to invoke new light particles in the thermal plasma coupled to the Higgs [16,

¹This different behaviour is not needed in (peculiar) setups where the EWPT is preceded by some exotic phenomena. One example is the warped extradimension framework in which the EWPT is forbidden till when the deposite-composite transition starts [6–9]. A further case occurs when inflation has a reheating temperature below the EW scale [10–15].

17]. In general, making these new light fields naturally compatible with the present LHC constraints requires to rely on either extra symmetries or particular parameter regions. The strategies to test these scenarios are therefore very model dependent. However, new light particles are not a necessary ingredient to achieve a SFOEWPT. Higher-dimensional operators, obtained by integrating out heavy fields, can also provide large non-SM contributions to the Higgs potential. In this case, the lack of observation of additional particles would not be ascribed to circumstantial conditions, but simply to a considerable gap between the EW scale and the new physics scale, f .

At the EW scale, the theory with $\mathcal{O}(f)$ -mass fields can be described by an effective Lagrangian containing the SM interactions as well as a tower of effective operators suppressed by powers of $1/f$. Among these operators, the interactions $\mathcal{O}_n = (\phi^\dagger \phi)^{\frac{n}{2}}$ have a radical impact on the Higgs potential (here ϕ is the Higgs EW doublet and n an even integer larger than four). Remarkably, if the coefficients of \mathcal{O}_n are sizeable, the EWSB occurs via a SFOEWPT [18–23].

Contrary to other operators, the only relevant signature of \mathcal{O}_n at colliders is the modification of the double- and triple-Higgs production rates. In SM searches, this is equivalent to measuring the Higgs self-coupling λ_3 . However, the LHC capabilities for probing the latter are weak. Even at the end of the High-Luminosity (HL) run, the LHC will be sensitive only to $-0.7 \lesssim \Delta\lambda_3/\lambda_3^{SM} \lesssim 7.1$ [24–26]. Due to this insensitivity, no relevant limits on \mathcal{O}_n can be ever put by the LHC. This is unfortunate because an accurate measurement of the Higgs self-coupling would allow to bound \mathcal{O}_n and thus shed light on the nature of the EWPT. We must wait for the ILC or the FCC to test a SM-like λ_3 with an accuracy of the order of 10 % via multi-Higgs production [25, 27]. Nevertheless, as we conclude in the present article, we may not have to wait for these future colliders to decipher whether the heavy physics compatible with the SFOEWPT exists.

To reach the above conclusion, we first consider, in section 2, weakly-coupled UltraViolet (UV) completions of the SM that induce \mathcal{O}_6 . It turns out that, with the exception of a custodial scalar quadruplet —whose phenomenology we study in detail and which becomes testable in multi-lepton signals at the LHC— most of the setups generate other effective operators that are very constrained, unless the couplings involved are fine-tuned. Moreover, we also notice that not including higher dimensional operators in the potential reduces substantially the validity of the Effective Field Theory (EFT). Hence, we focus subsequently on the next-to-minimal SM EFT, which includes both \mathcal{O}_6 and \mathcal{O}_8 . This is also argued to describe strongly-coupled UV completions, because in this case, both operators often emerge with large coefficients.

Section 3 presents the analysis of the EWPT in this extended EFT. Here we accurately determine the regions of the parameter space leading to the SFOEWPT. Moreover, we analyse the validity of the mean-field approximation. We also identify the precise values of the coefficients of \mathcal{O}_6 and \mathcal{O}_8 that LISA can test.

In section 4 we summarise the reach of the LHC and future colliders to the modified Higgs couplings, and we reinterpret them in terms of the \mathcal{O}_6 and \mathcal{O}_8 coefficients. We also compare to the LISA sensitivity. In addition, we comment on the implications of having further operators

affecting sectors other than the Higgs potential. Finally, section 5 is dedicated to summarise the main results of the paper and the consequent conclusions.

2 A gap between the standard model and new physics

We consider the EFT of extended Higgs sectors. The effective Lagrangian after integrating out the new degrees of freedom reads

$$L = L_{\text{SM}} + \sum_i \frac{c_i}{f^{4-d_i}} \mathcal{O}_i , \quad (2.1)$$

where L_{SM} stands for the SM Lagrangian, c_i/f^{4-d_i} represents the coefficient of the corresponding operator \mathcal{O}_i and f is the typical new-physics scale. The couplings are all expected to scale as $c_i \sim \tilde{g}^2 \times \tilde{g}^{2n}/(4\pi)^{2n}$, with \tilde{g} some weak coupling, n the perturbative order at which \mathcal{O}_i is generated, and d_i the canonical dimension of \mathcal{O}_i .

As we will detail in section 3, the scalar potential is compatible with a SFOEWPT only if some of the dimension-six couplings are of $\mathcal{O}(1)$ TeV⁻². In a weakly-coupled theory, only the operators of dimension six produced at tree level can be expected to be so large. Interestingly, in a Warsaw-like basis [28], such operators entering the (tree-level) Higgs potential amount to only a few and, for an UV theory involving exclusively new scalars, they are [29]²

$$\mathcal{O}_6 = (\phi^\dagger \phi)^3 , \quad \mathcal{O}_{d6} = \frac{1}{2} \partial_\mu (\phi^\dagger \phi) \partial^\mu (\phi^\dagger \phi) , \quad \mathcal{O}_{\phi D} = (\phi^\dagger D_\mu \phi) ((D^\mu \phi)^\dagger \phi) , \quad (2.2)$$

with ϕ being the Higgs doublet. These typically appear together with further effective interactions. The same scalars generating $\mathcal{O}_6, \mathcal{O}_{d6}$ and $\mathcal{O}_{\phi D}$ also induce, at the same order, the operators

$$\mathcal{O}_{\psi\phi} = y_\psi (\phi^\dagger \phi) (\bar{\psi}_L \phi \psi_R) , \quad (2.3)$$

with y_ψ the Yukawa coupling of the SM fermions, here generically indicated as ψ_L and ψ_R . These operators modify the Higgs-fermion interactions.

We anticipate that $\mathcal{O}_{\psi\phi}$ have little relevance for the subsequent discussion because present measurements constrain the deviations from the SM induced by them to be at or below 10% [32]. On the contrary, it is well known that \mathcal{O}_6 is poorly bounded and plays a major role in the modifications to the SM scalar potential and, hence, in the EWPT. The custodially-breaking operator $\mathcal{O}_{\phi D}$ can be forced to be negligible at the matching scale by enforcing selection rules (*i.e.* a symmetry), but it can still have a strong impact at low scales due renormalization group effects. Finally, \mathcal{O}_{d6} is in general also present, although severely constrained.

²Note that \mathcal{O}_6 is crucial for the SFOEWPT and cannot be originated from integrating out at tree level new fermions [29–31]. We also stress that the operator basis in Eq. (2.2) is converted into the proper Warsaw basis [28] by integrating by parts \mathcal{O}_{d6} .

2.1 Thermal effects of \mathcal{O}_6 on the electroweak phase transition

It is well known that \mathcal{O}_6 is sufficient to allow for a SFOEWPT [18–23]. For this to happen without any other higher-dimensional operator contribution, the value of c_6/f^2 must be $\mathcal{O}(1)$ TeV^{−2}. In the present section we show how this order of magnitude can be obtained. Being ours an order-of-magnitude estimate, we limit ourselves to calculating all relevant quantities at the critical temperature (instead of the nucleation temperature; see section 3). We moreover neglect all higher-dimensional operators but \mathcal{O}_6 in the loop effects, and we account for \mathcal{O}_{d6} only via its role in the tree-level Higgs observables. The impact of $\mathcal{O}_{\psi\phi}$ and $\mathcal{O}_{\phi D}$ on the EWPT is totally neglected. These approximations are further justified because, as explained in the introduction, we are particularly interested in the parameter region that cannot be discovered at the LHC and, at the end of the HL run, the values of $c_{d6}, c_{\phi D}$ and $c_{\psi\phi}$ will be too constrained to have a relevant role in the EWPT; see also section 2.2.

The SMEFT Lagrangian we are dealing with contains the following kinetic term and potential for the field \tilde{h} belonging to the doublet $\phi = [G^+, (\tilde{h} + i G^0)/\sqrt{2}]^t$:

$$K = \frac{1}{2} \left(1 + \frac{c_{d6} \langle \tilde{h} \rangle^2}{f^2} \right) \partial_\mu \tilde{h} \partial^\mu \tilde{h} , \quad (2.4)$$

$$V(\tilde{h}) = -\frac{\mu^2}{2} \tilde{h}^2 + \frac{\lambda}{4} \tilde{h}^4 + \frac{c_6}{8 f^2} \tilde{h}^6 , \quad (2.5)$$

where all derivative interactions have been omitted. Notice that $\langle \tilde{h} \rangle$, which is the Vacuum Expectation Value (VEV) of \tilde{h} in the EW broken phase, can be fixed to $v = 246$ GeV because we are neglecting $\mathcal{O}_{\phi D}$ and therefore the W and Z gauge boson masses are $m_W^2 = g^2 \langle \tilde{h} \rangle^2 / 4$ and $m_Z^2 = (g^2 + g'^2) \langle \tilde{h} \rangle^2 / 4$, with g and g' the SM $SU(2)_L$ and $U(1)_Y$ gauge couplings.

We set now the parameters of the scalar potential. In the broken phase, we have $\tilde{h} = \langle \tilde{h} \rangle + \eta$. However, η is not yet canonically normalised according to Eq. (2.4). We therefore trade η by defining the correctly normalised field h as

$$h = \eta \sqrt{1 + c_{d6} \frac{v^2}{f^2}} = \eta \sqrt{\omega} . \quad (2.6)$$

Then, we use the inputs $m_h \sim 125$ GeV and $\langle \tilde{h} \rangle = v$ to express μ^2 and λ as a function of c_6/f^2 and c_{d6}/f^2 . We obtain

$$\mu^2 = \frac{m_h^2}{2} + \frac{v^2}{f^2} \left(\frac{1}{2} c_{d6} m_h^2 - \frac{3}{4} c_6 v^2 \right) , \quad \lambda = \frac{m_h^2}{2v^2} + \frac{v^2}{f^2} \left(\frac{c_{d6}}{2} \frac{m_h^2}{v^2} - \frac{3c_6}{2} \right) . \quad (2.7)$$

To ensure the stability of the EW minimum, we also impose $c_6 > 0$. This condition, together with Eq. (2.7), is indeed sufficient to guarantee the stability of the potential up to scales below the cutoff f , around and above which the EFT description breaks down³.

³The present EFT approach is consistent only at energy scales Q such that $g_i Q^2 / f^2 \ll 1$. Questioning the behaviour of the potential at higher scales, like its stability, is feasible only when the UV completion is specified.

In order to evaluate the critical temperature of the EWPT, T_c , we adopt the mean-field approximation and consider only the c_6 's effects in the radiative corrections. Within these approximations (in particular up to loop corrections proportional to c_{d6}) the one-loop thermal potential of h turns out to be [21, 33]

$$V(h, T) = \frac{-\mu^2 + a_0 T^2}{2} \left(v_T + \frac{h}{\sqrt{\omega}} \right)^2 + \frac{\lambda}{4} \left(v_T + \frac{h}{\sqrt{\omega}} \right)^4 + \frac{c_6}{8 f^2} \left(v_T + \frac{h}{\sqrt{\omega}} \right)^6 \quad (\text{mean-field approximation}) , \quad (2.8)$$

with $a_0 = \frac{1}{16} \left(4 \frac{m_t^2}{v^2} + 3g^2 + g'^2 + 4y_t^2 - 12c_6 \frac{v^2}{f^2} \right)$ and $y_t = \sqrt{2} m_t / \langle \tilde{h} \rangle$, where m_t is the top mass. Moreover v_T is the VEV of the Higgs at the temperature T .

By definition, at $T = T_c$, the EW symmetry breaking and conserving minima are degenerate, with the corresponding finite-temperature VEVs being $\langle h \rangle = 0$ and $\langle h \rangle = -\sqrt{\omega} v_{T_c}$, respectively. Their degeneracy implies [33]⁴

$$\lambda^2 = 4(-\mu^2 + a_0 T_c^2) \frac{c_6}{f^2} , \quad v_{T_c}^2 = -\frac{\lambda}{c_6} f^2 \quad (\text{mean-field approximation}) . \quad (2.9)$$

Thus, equating λ from Eq. (2.7) and Eq. (2.9) yields

$$\frac{c_6}{f^2} = \frac{m_h^2}{v^2(3v^2 - 2v_{T_c}^2)} \left(1 + \frac{c_{d6} v^2}{f^2} \right) , \quad (2.10)$$

which, by means of Eqs. (2.7) and (2.9) again, leads to

$$T_c^2 = \frac{3c_6}{4a_0 f^2} (v^2 - v_{T_c}^2) (v^2 - \frac{1}{3} v_{T_c}^2) . \quad (2.11)$$

Since T_c^2 must be positive, we have either $v_{T_c}^2 > 3v^2$ or $v_{T_c}^2 < v^2$. The latter is equivalent to

$$\frac{m_h^2}{3v^4} \left(1 + \frac{c_{d6} v^2}{f^2} \right) < \frac{c_6}{f^2} < \frac{m_h^2}{v^4} \left(1 + \frac{c_{d6} v^2}{f^2} \right) , \quad (2.12)$$

while the former is not physical for a potential like the one in Eq. (2.8). Note that in the limit $c_{d6} \rightarrow 0$ we reproduce the results of Ref. [33].

Within our approximations, when c_6/f^2 satisfies the constraints in Eq. (2.12), the EWPT is of first order. This condition does not precisely imply the so-called out-of-equilibrium requirement for EW baryogenesis. For this baryogenesis mechanism it is indeed crucial that the first order EWPT is, in addition, strong, *i.e.* that the EW sphalerons are out of equilibrium in the broken phase at $T = T_n$, the temperature at which the EWPT occurs. In practice, this situation is achieved if $2 m_W(T_n) \gtrsim g T_n$, with $m_W(T_n) = g v_{T_n}/2$. For a rough identification of the SFOEWPT parameter region, it however suffices to investigate the condition $2 m_W(T_c) \gtrsim$

⁴As expected, for $c_6 > 0$ the mean-field approximation shows that the SFOEWPT is possible only if $\lambda < 0$. This is not the case when the full finite-temperature contribution is taken into account; see section 3.

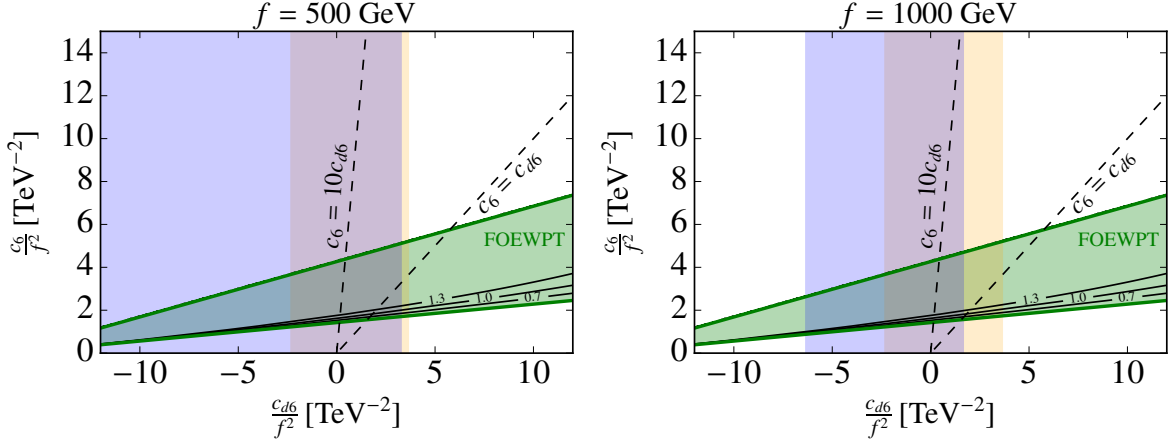


Figure 1. The LHC and SFOEWPT constraints on the $c_6 - c_{d6}$ parameter space for $f = 500$ GeV and $f = 1$ TeV. The green band highlights the region where the mean-field approximation hints at a first EWPT. Above this band the EW breaking minimum is above the symmetric one, while below the EWPT is not of first order. The black solid lines mark the contours $v_{T_c}/T_c = 0.7, 1.0$ and 1.3 . In the yellow and blue areas c_{d6} is consistent with the bounds in Eq. (2.16) and Eq. (2.15), respectively.

gT_c , or equivalently $v_{T_c}/T_c \gtrsim 1$ [16, 34]⁵. In such a case, the values of c_6 and c_{d6} leading to a SFOEWPT can be determined from Eqs. (2.9) and (2.10).

Figure 1 displays the $c_6/f^2 - c_{d6}/f^2$ parameter region (green area) where the condition in Eq. (2.12) is satisfied. Above the green area (*cf.* upper bound in Eq. (2.12)), the EW symmetry breaking is not feasible since the EW breaking minimum is above the symmetric one. The solid lines labelled as 0.7, 1.0 and 1.3 mark the lower bound on c_6/f^2 for allowing $v_{T_c}/T_c > 0.7, 1$ and 1.3 , respectively. These lines are quite close one each other, hinting at the fact that the ballpark of the c_6/f^2 and c_{d6}/f^2 values achieving the SFOEWPT is not very sensitive to the precise calculation of v_{T_c} and T_c ⁶.

All together, it can be seen that large values of c_6 are needed, and so large coefficients for the other operators in Eq. (2.2) are expected from a bottom-up point of view. This contrasts with the current bounds from the LHC (yellow and blue areas), which we describe in the next section.

⁵A comparison of the findings due to $v_{T_c}/T_c \gtrsim 1$ versus $v_{T_n}/T_n \gtrsim 1$ is presented in section 3. Note that also the bound $v_{T_n}/T_n \gtrsim 1$ should be considered indicative as several other effects can influence it [35–39].

⁶As a last remark, we comment on the values of the coefficients c_i that enter the above calculation. Whereas a renormalization-group improved calculation of the Higgs potential would have been sensitive to the running of the parameters (see *e.g.* Refs. [40, 41] for an explicit application), in the present estimate the values of the couplings that are relevant are exclusively the tree level ones. For practical purposes, we can thus assume that the values of c_i we have used, are those at the matching scale f and thus are not precisely those relevant for the LHC phenomenology.

2.2 Current LHC constraints

Due to the LHC insensitivity to \mathcal{O}_6 , the most promising searches to test the above c_6/f^2 – c_{d6}/f^2 parameter region compatible with a SFOEWPT, are those sensitive to \mathcal{O}_{d6} .

As previously discussed, \mathcal{O}_{d6} provides a contribution to the Higgs kinetic term. Such a correction can be absorbed into the field redefinition of Eq. (2.6). As a consequence, the Higgs couplings to fermions and gauge bosons are modified with respect to those of the SM by the factors ⁷

$$\frac{g_{hff}}{g_{hff}^{\text{SM}}} = c, \quad \frac{g_{hVV}}{g_{hVV}^{\text{SM}}} = a, \quad \frac{g_{hgg}}{g_{hgg}^{\text{SM}}} = c, \quad \frac{g_{h\gamma\gamma}}{g_{h\gamma\gamma}^{\text{SM}}} = \frac{aI_\gamma + cJ_\gamma}{I_\gamma + J_\gamma}, \quad (2.13)$$

with

$$a = 1 - c_{d6} \frac{v^2}{2f^2}, \quad c = 1 - c_{d6} \frac{v^2}{2f^2} + \mathcal{O}(c_{\psi\phi}, c_{\phi D}) \frac{v^2}{f^2}, \quad (2.14)$$

and $I_\gamma \simeq -1.84$, $J_\gamma \simeq 8.32$. According to the discussion in the previous section, we could safely neglect the contribution of $\mathcal{O}_{\psi\phi}$ and $\mathcal{O}_{\phi D}$ to c . Here, instead, we just obtain robust constraints on c_{d6} from the present LHC measurements by marginalising the Run-1 constraints on a over all possible values of c . One obtains [42]

$$c_{d6} \frac{v^2}{2f^2} = 0.02 \pm 0.09 \quad \text{at 68\% C.L.} \quad (2.15)$$

Likewise, repeating the same procedure with the current constraints improves this bound to ± 0.06 . A further improvement to ± 0.03 is expected at the end of the HL run if no new physics is found [32]. In Fig. 1, the parameter region compatible with the Run 1 bound is shown in yellow.

We also note that neglecting $\mathcal{O}_{\phi D}$ can be justified at the matching scale, since $c_{\phi D}(f) \approx 0$ can be naturally explained by means of UV symmetries. However, due to \mathcal{O}_{d6} , $c_{\phi D}$ runs between the renormalization scales f and v [43]:

$$c_{\phi D}(v) \simeq c_{\phi D}(f) + \frac{5}{24\pi^2} g'^2 c_{d6}(f) \log \frac{f}{v}. \quad (2.16)$$

The present constraint on the coupling of $\mathcal{O}_{\phi D}$, namely [44]

$$-0.023 < c_{\phi D}/f^2 \text{ TeV}^2 < 0.006, \quad (2.17)$$

provides an (indirect) bound on c_{d6} and, in turn, on the SFOEWPT parameter region we have calculated. The corresponding constraint is presented in blue in Fig. 1. This constraint on c_{d6} does depend on the value of the EFT cutoff f . Of course, at the end of the HL run, the SFOEWPT area not tested via $\mathcal{O}_{\phi D}$ effects will be much smaller.

⁷In a complete dimension-six analysis, there are even more operators contributing to these factors, like $G_{\mu\nu} G^{\mu\nu} \phi^\dagger \phi$ and a similar operator for the photon. These can also be constrained by Higgs-couplings measurements and they do not contribute to the EWPT at tree level.

In conclusion, the SFOEWPT parameter region overcoming the considered constraints requires

$$1 \lesssim c_6/f^2(1\text{TeV})^2 \lesssim 5\kappa \quad (c_{d6} \text{ within the current bounds}) , \quad (2.18)$$

with $\kappa = 1$. (The results in section 3 will change κ to around 0.5.) The lower (upper) bound is allowed for $c_{d6}/f^2 \approx 3.5 \text{ TeV}^{-2}$ ($c_{d6}/f^2 \approx -5 \text{ TeV}^{-2}$) and has a slight dependence on f . These will be more stringent if the LHC does not detect deviations from the SM at the end of HL run. In the extreme case of imposing $c_{d6} = 0$, the SFOEWPT parameter region reduces to

$$1.7 \lesssim c_6/f^2(1\text{TeV})^2 \lesssim 4\kappa \quad (\text{for } c_{d6} = 0) , \quad (2.19)$$

in agreement with Ref. [19].

Clearly, in view of the aforementioned LHC bounds on c_{d6} and $c_{\phi D}$ and the limits in Eqs. (2.12) and (2.19), there will be little room for these couplings to be of the size of c_6 , as suggested by power counting estimates in weakly-coupled scenarios; see dashed black lines in Fig. 1. It is therefore crucial to understand whether there exist concrete UV scenarios that, at low energy, naturally generate a large hierarchy between c_6 and the other c_i coefficients.

2.3 Concrete realizations

In light of the above discussion, it is worth considering scenarios in which operators other than \mathcal{O}_6 are negligible. To this aim, let us first assume that the SM Higgs sector is extended only with new heavy scalars with isospin $I \leq 1$; see Ref. [30] for a related discussion. Concrete realisations and their signals at lepton colliders have been also discussed in Ref. [45]. In the simplest case in which there is only one new field, φ , \mathcal{O}_6 is the only operator generated at tree level if and only if φ is a colourless $SU(2)_L$ doublet with vanishing couplings to the fermions [29, 46]. This scenario is then poorly motivated, because there is no symmetry that can remove *only* the doublet couplings to fermionic currents, since a \mathbb{Z}_2 parity under which they are the only odd fields would make c_6 also vanish. Moreover, the new doublets appearing in the most common UV setups do not exhibit this property.

On the other hand, one might argue that many motivated extensions of the SM Higgs sector involve several new fields. This is for instance the case of non-minimal composite Higgs models⁸. One particularly interesting example is the coset $SU(5)/SO(5)$ [48], which admits a four-dimensional UV completion [49]. The scalar sector consists of a hyperchargeless triplet, Ξ_0 , a triplet with hypercharge 1, Ξ_1 , and a neutral singlet \mathcal{S} on top of the Higgs doublet. The

⁸We note that composite Higgs models involve strongly-coupled dynamics and they are better described by the EW chiral Lagrangian; see section 2.5. However, it has been shown that, in certain parameter space regions, the contribution of the extra scalars to the Higgs effective operators can overcome the contribution of the strong sector [47].

effective operators we are interested in receive multiple contributions, namely

$$\frac{c_{d6}}{f^2} = \frac{1}{M^4} \left(\kappa_S^2 - \kappa_{\Xi_0}^2 - 4|\kappa_{\Xi_1}|^2 \right), \quad \frac{c_{\phi D}}{f^2} = -\frac{2}{M^4} \left(\kappa_{\Xi_0}^2 - 2|\kappa_{\Xi_1}|^2 \right), \quad (2.20)$$

$$\frac{c_{\psi\phi}}{f^2} = \frac{1}{M^4} \left(\kappa_{\Xi_0}^2 + 2|\kappa_{\Xi_1}|^2 \right), \quad (2.21)$$

and

$$\begin{aligned} \frac{c_6}{f^2} = & \frac{\kappa_S}{M^4} \left(-\lambda_S \kappa_S + \frac{\kappa_S^3 \kappa_S^2}{M^2} - \lambda_{S\Xi_0} \kappa_{\Xi_0} - 4 \operatorname{Re} [\lambda_{S\Xi_1} (\kappa_{\Xi_1})^*] + \frac{\kappa_{S\Xi_0} \kappa_{\Xi_0}^2}{M^2} + \frac{2\kappa_{S\Xi_1} |\kappa_{\Xi_1}|^2}{M^2} \right) \\ & - \frac{\kappa_{\Xi_0}^2}{M^4} (\lambda_{\Xi_0} - 2\lambda) - \frac{|\kappa_{\Xi_1}|^2}{M^4} \left(2\lambda_{\Xi_1} - \sqrt{2} \tilde{\lambda}_{\Xi_1} - 4\lambda \right) - \frac{2\sqrt{2}}{M^4} \operatorname{Re} [\lambda_{\Xi_1\Xi_0} (\kappa_{\Xi_1})^* \kappa_{\Xi_0}] \\ & - \frac{\sqrt{2}}{M^6} \kappa_{\Xi_0\Xi_1} \kappa_{\Xi_0} |\kappa_{\Xi_1}|^2, \end{aligned} \quad (2.22)$$

where M is the (assumed common) mass term of all new scalars, and the other couplings just parameterise the renormalizable interactions among themselves and the SM particles [29].

It is interesting to show that not even in this case, which contains several scalars and many different couplings, can \mathcal{O}_6 be the only non-vanishing operator. Indeed, $c_{\phi D}$ only vanishes for $\kappa_{\Xi_0} = \sqrt{2}|\kappa_{\Xi_1}|$. This choice can in fact be enforced by an $SU(2)_L \times SU(2)_R$ symmetry, as in the Georgi-Machacek model [50]. It would yield

$$\frac{c_{d6}}{f^2} = \frac{1}{M^4} \left(\kappa_S^2 - 6|\kappa_{\Xi_1}|^2 \right), \quad (2.23)$$

which could then be removed by enforcing $\kappa_S = \sqrt{6}|\kappa_{\Xi_1}|$. As a result, it would turn out that $c_{\psi\phi}/f^2 = 4|\kappa_{\Xi_1}|^2/M^4$, which vanishes if and only if $\kappa_{\Xi_1} = 0$. In such a case, however, c_6 is vanishing too.

Actually, we can go further and show that *there is no weakly-coupled renormalizable extension of the Higgs sector containing singlets or triplets —with non-vanishing couplings to the SM— in which the effective operators produced after integrating out all new scalars at tree level modify only the scalar potential*.

In order to prove this statement, let us work in the Warsaw basis and use the results of Ref. [29]. Let us also assume first that the extended Higgs sector contains (at least) one neutral singlet. This field generates a positive c_{d6} that can be only cancelled by the contribution of a colourless triplet scalar. Indeed, any combination of colourless-triplet scalars, independently of the number of fields and their quantum numbers, gives a negative contribution to c_{d6} . This contribution is in fact the sum of all independent contributions [29].

Colourless triplet scalars, on their side, also produce the operator $\mathcal{O}_{\psi\phi}$ with coefficient $c_{\psi\phi} \propto c_{d6}$. Therefore, it cannot be neglected if the triplet has to cancel the singlet contribution to \mathcal{O}_{d6} . The operator $\mathcal{O}_{\psi\phi}$, in turn, cannot be cancelled by the singlet, which does not produce it at all at tree level. For this matter, at least one extra doublet is to be present, too. However, doublets produce also four-fermion operators like $\mathcal{O}_{le} = (\bar{l}_L \gamma_\mu l_L)(\bar{e}_R \gamma^\mu e_R)$. This is actually

generated only by doublets, with negative sign for l_L and e_R of the same flavour. So, it cannot be removed at all by including other scalar fields. Instead, its coefficient must be explicitly forced to vanish. In such a case, however, the coupling $c_{\psi\phi}$ induced by the triplets would be strictly vanishing, and so all the linear interactions between the new physics and the SM, in contradiction with our hypothesis. Had we started considering the presence of at least one triplet, instead of one singlet, we would have arrived to exactly the same conclusion.

Let us now consider the case $I > 1$. The only scalars that can couple in a renormalizable way to the SM sector are quadruplets with hypercharges $Y = 1/2, 3/2$. Interestingly, they contribute only to \mathcal{O}_6 when integrated out. These quadruplets can appear, for example, in Grand Unified Theories (GUT).

In GUT models, the SM fermions as well as the Higgs doublet are embedded in multiplets of a simple gauge group containing the SM $SU(3)_c \times SU(2)_L \times U(1)_Y$. Two main GUT gauge groups have been typically considered in the literature, namely $SU(5)$ and $SO(10)$ (and at a lesser extent, $E_6 \supset SO(10) \supset SU(5)$). The minimal irreducible representations of the scalar fields that can lead to SM gauge uncoloured quadruplets are the **35** and the **70** in $SU(5)$ [51, 52].

Obviously, such large-dimensional representations do not decompose only into quadruplets, but into many other states. An example is

$$\mathbf{35} = (\mathbf{1}, \mathbf{4})_{3/2} + (\bar{\mathbf{3}}, \mathbf{3})_{2/3} + (\bar{\mathbf{6}}, \mathbf{2})_{1/6} + (\bar{\mathbf{10}}, \mathbf{1})_1, \quad (2.24)$$

where the two numbers in parenthesis and the sub-index denote the dimension of the irreducible representation of $SU(3)_c$ and $SU(2)_L$ under which the corresponding field transforms and its hypercharge, respectively. Clearly, larger representations reduce to a larger number of exotic fields. Despite being unlikely, it is still possible that the effective operators generated by the coloured scalars are sub-leading with respect to the \mathcal{O}_6 induced by the quadruplet. This can happen in two cases: *i*) If the coloured scalars are much heavier (which can be justified if a specific mechanism, similar to those advocated to solve the doublet-triplet splitting problem in SUSY GUT models [53–58], is enforced); *ii*) if all non-quadruplet fields have vanishing linear couplings to the SM at the renormalizable level. Surprisingly, this is the case for all extra fields in Eq. (2.24) (although in principle they could couple, *e.g.*, to dangerous flavour-violating currents via effective interactions).

Although the representation **35** does not include the Higgs boson, nor is required to break $SU(5)$ down to the SM gauge group (unlike *e.g.* the **24**), the aforementioned observations motivate further studies of a Higgs sector extended with a quadruplet⁹. The next section is devoted to investigate in some detail UV completions involving quadruplets.

⁹Larger representations, such as the mentioned **70**, do contain a Higgs doublet, but also other fields with renormalizable interactions to the SM fermions. Moreover, smaller representations typically contain singlets and triplets (such as in the **15** and the **24**, to name a few).

2.4 Phenomenology of quadruplets

As previously noticed, among all possible dimension-six operators, at tree level the scalar $SU(2)_L$ quadruplets with $Y = 1/2, 3/2$ induce only operators of the scalar potential. Other effects are therefore suppressed by higher powers of $1/M^2$, being M the mass of these fields. Inspired by Eq. (2.24), we first explore the case $Y = 3/2$ in some detail. Then, motivated by the findings, we explore a setup where both $Y = 1/2$ and $Y = 3/2$ quadruplets are present.

2.4.1 The SM plus a $Y = 3/2$ quadruplet

The scalar potential of the SM plus a $Y = 3/2$ quadruplet is given by

$$V = \mu^2 \phi^\dagger \phi + \mu_{\Theta_3}^2 \Theta_3^\dagger \Theta_3 + \lambda (\phi^\dagger \phi)^2 + \lambda_2 (\Theta_3^\dagger \Theta_3)^2 \\ + \lambda' (\phi^\dagger \phi) (\Theta_3^\dagger \Theta_3) + \tilde{\lambda} (\phi^\dagger \tau_a \phi) (\Theta_3^\dagger T_a \Theta_3) + \left(\lambda_{\Theta_3} \phi^3 \Theta_3^\star + \text{h.c.} \right), \quad (2.25)$$

with τ_a and T_a being the $SU(2)_L$ generators in the two- and four-dimensional representations; see *e.g.* Ref. [59–61] for explicit expressions and phenomenological studies. For our aims, all parameters can be considered as real. Notice that the last interaction term is the responsible for \mathcal{O}_6 at low energy:

$$\lambda_{\Theta_3} \phi^3 \Theta_3^\star \equiv \lambda_{\Theta_3} (\phi^\dagger \sigma_a \tilde{\phi}) C_{a\beta}^I \tilde{\phi}_\beta \epsilon_{IJ} \Theta_3^J \quad \Longrightarrow \quad c_6 = \frac{3}{2} \frac{\lambda_{\Theta_3}^2}{\mu_{\Theta_3}^2}. \quad (2.26)$$

In this equation, $\beta = 1/2, -1/2$, $a = 1, 2, 3$ and $I, J = -3/2, -1/2, 1/2, 3/2$. The only non-vanishing Clebsh-Gordan coefficients in $C_{a\beta}^I$ are $C_{1,1/2}^{3/2} = -C_{1,-1/2}^{-3/2} = iC_{2,1/2}^{3/2} = iC_{2,-1/2}^{-3/2} = 1/\sqrt{2}$, and $C_{3,-1/2}^{-1/2} = C_{3,1/2}^{1/2} = 2C_{1,1/2}^{-1/2} = -2C_{1,-1/2}^{1/2} = -2iC_{2,1/2}^{-1/2} = -2iC_{2,-1/2}^{1/2} = -2/\sqrt{6}$. The quantity ϵ_{IJ} is the total anti-symmetric two-dimensional tensor.

In order to ensure that the SMEFT (with the quadruplet integrated out) can accurately describe the phase transition, we need the SMEFT to be a good description of the fundamental theory all along the tunnelling trajectory. This requires the quadruplet to be above the EW scale even when the Higgs has no VEV. We thus restrict ourselves to the case $\mu_{\Theta_3}^2 \gg m_Z^2$.

The main constrain on this scenario comes from the observed value of the ρ parameter [60, 61], $\rho_{tree} = (v^2 + 3v_{\Theta_3}^2)/(v^2 + 9v_{\Theta_3}^2)$, with v_Θ the VEV acquired by the quadruplet neutral component. The experimental bound $\rho_{exp} = (1.00037 \pm 0.00023)$ imposes $v_{\Theta_3}^2 \lesssim 0.9 \text{ GeV}^2$ at the 2σ level [62]. This in particular implies $|v v_{\Theta_3}| \ll M_{\Theta_3^0}^2 - m_h^2$, with $M_{\Theta_3^0}^2 \simeq \mu_{\Theta_3}^2 + [\lambda'/2 + 3\tilde{\lambda}/4]v^2$, such that the electrically-neutral CP-even components of the quadruplet and doublet do not mix appreciably, in agreement with the 125 GeV Higgs coupling measurements [63]. However, the tadpole equation coming from Eq. (2.25) yields

$$|v_{\Theta_3}| \simeq \frac{|\lambda_{\Theta_3}| v^3}{2M_{\Theta_3^0}^2} \simeq \frac{c_6}{f^2} \frac{v^3}{|\lambda_{\Theta_3}|}. \quad (2.27)$$

Therefore there is some tension between the ρ parameter bound and the SFOEWPT requirement of Eq. (2.19). Indeed, the ρ parameter is compatible at the 2σ level with this condition only for $\lambda_{\Theta_3} \gtrsim 10$, completely out of the perturbative unitarity limit $\sim \sqrt{4\pi}$.

2.4.2 A custodial quadruplet setup

We have just observed that EW precision data put the quadruplet scenario under tension, despite the heavy field only modifying the Higgs potential at tree level at dimension six. The reason is that corrections to the ρ parameter, which is very precisely measured, do appear at dimension eight by operators such as $\sim \lambda_{\Theta_3}(\phi^\dagger \phi)\mathcal{O}_{\phi D}$. These can be avoided in quadruplet extensions with custodial symmetry, as we discuss now.

The most economical scenario involves two EW quadruplets, Θ_1 and Θ_3 , with the same mass M and with hypercharges $Y = 1/2$ and $Y = 3/2$, respectively. They couple as $\phi^3 \Theta_1^\star = (\phi^\dagger \sigma_\alpha \phi) C_{\alpha\beta}^I \tilde{\phi}_{\beta\epsilon IJ} \Theta_1^J$ and $\phi^3 \Theta_3^\star$ (see Eq. (2.26)) with strengths λ_Θ and $\sqrt{3}\lambda_\Theta$, respectively, with λ_Θ a free parameter. Custodial symmetry also enforces the neutral components of both quadruplets to take the same VEV $\langle \Theta_1^0 \rangle = \langle \Theta_3^0 \rangle = v_\Theta$. This VEV breaks $SU(2)_L \times SU(2)_R \rightarrow SU(2)_V$. It can be trivially checked that $\rho = 1$ at tree level. (Note that Θ_1^0 and Θ_3^0 have different third-component isospin.) At low energies, c_6 is the sum of the contributions of both quadruplets, namely

$$c_6 = \frac{1}{2} \frac{\lambda_\Theta^2}{M^2} + \frac{9}{2} \frac{\lambda_\Theta^2}{M^2} = 5 \frac{\lambda_\Theta^2}{M^2} . \quad (2.28)$$

We have also checked, using SARAH [64], that loop corrections to the ρ and S parameters are well within the experimental bound. The collider phenomenology of the custodial quadruplet can be understood in terms of the unbroken $SU(2)_V$. The Higgs bi-doublet decomposes as $(\mathbf{2}, \mathbf{2}) = 1 + \mathbf{3}$, while the custodial bi-quadruplet decomposes as $(\mathbf{4}, \mathbf{4}) = 1 + \mathbf{3} + \mathbf{5} + \mathbf{7}$. The latter singlet and triplet contain only electrically neutral and singly-charged scalars, which are difficult to produce and detect at colliders. Note that they only couple to the SM fermions via the mixing with the Higgs singlet and triplet. Moreover, this mixing is very small: After all, \mathcal{O}_6 is the only operator generated at tree level, which does not modify the Higgs couplings at low energy. This also suggests that measuring the Higgs couplings is not the most promising strategy to test this setup.

Moreover, the septuplet contains large electric charges. However, these cannot directly decay into pairs of SM particles¹⁰. They decay only via the emission of (soft) gauge bosons into lower-charged states in the custodial quadruplet, which are also difficult to test at colliders. The quintuplet, instead, can be both efficiently produced (in pairs via EW interactions) and decays mostly into pairs of gauge bosons (indeed $\mathbf{3} \times \mathbf{3} = 1 + \mathbf{3} + \mathbf{5}$). Decays into pairs of Higgs bosons are not allowed, because this is a complete singlet of $SU(2)_V$. In particular, the doubly-charged, singly-charged and neutral components of the quintuplet decay with branching ratios

$$\text{Br}(\Theta^{\pm\pm} \rightarrow W^\pm W^\pm) = 1, \quad \text{Br}(\Theta^\pm \rightarrow W^\pm Z) = 1, \quad \text{Br}(\Theta^0 \rightarrow W^+ W^- + ZZ) = 1 . \quad (2.29)$$

We implement this model in MadGraph v5 [65] by means of Feynrules v2 [66]. We subsequently compute the pair-production cross sections mediated by neutral and charged

¹⁰Note that there is no $SU(2)_V$ septuplet constructed out of two 1 and/or two $\mathbf{3}$. The septuplet cannot even decay into three triplets: Although allowed by $SU(2)_V$, operators mediating this decay would contain at least three gauge bosons and one scalar, while Lorentz invariance forbids this kind of interaction at dimension four.

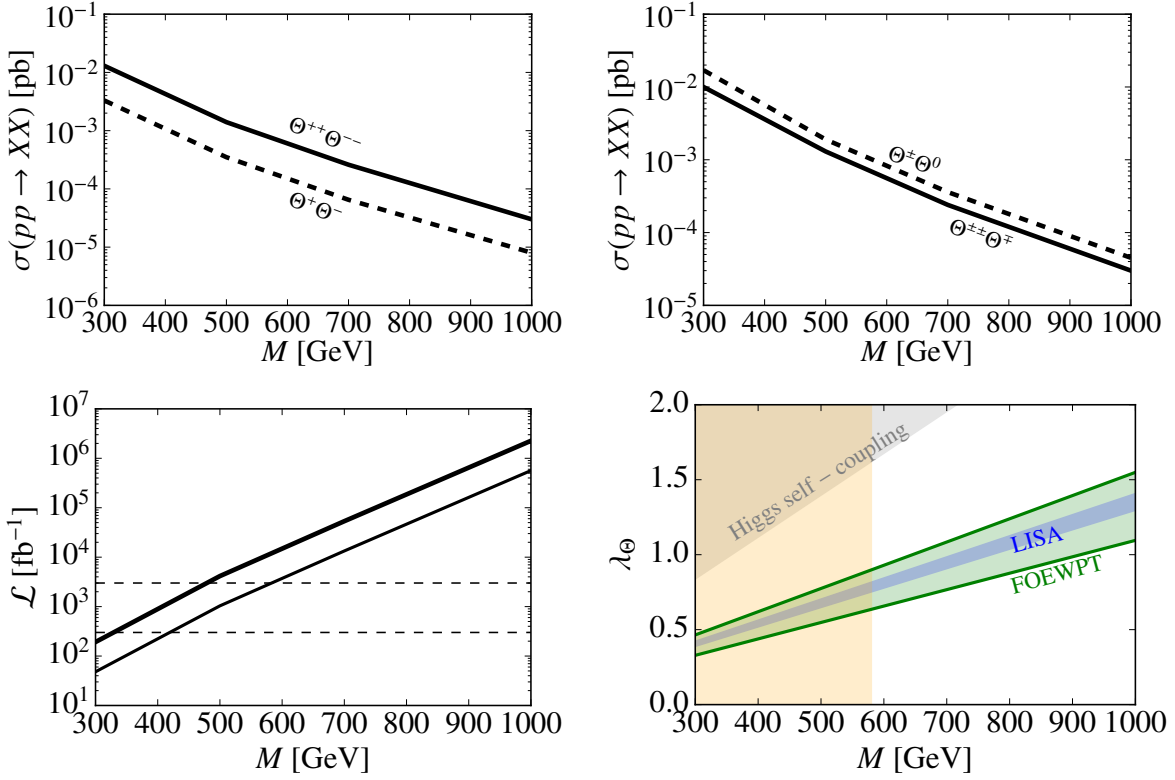


Figure 2. Upper left) Neutral current cross sections for pair-production of scalars in the custodial quadruplet model. Upper right) Same as before but for the charged current. Bottom left) Integrated luminosity required to exclude the custodial quadruplet at the 95 % C.L. for different masses using two different analyses; see text for details. Two representative values of the collected luminosity, $\mathcal{L} = 300 \text{ fb}^{-1}$ and $\mathcal{L} = 3 \text{ ab}^{-1}$ are also shown with dashed lines. Bottom right) Parameter space region where the FOEWPT takes place and the reach of different searches. The yellow region shows the HL-LHC reach taken from the bottom-left panel.

currents for masses in between 300 and 1000 GeV. The results are shown in the upper left and upper right panels of Fig. 2, respectively.

We have also estimated the current and the future LHC reach for this scenario. To this aim, we have generated Monte Carlo events, including radiation, fragmentation and hadronization effects with `Pythia v6` [67], and analysed them using `CheckMate v2` [68]. The latter implements several multi-lepton SUSY searches. Among them, the search that turns out to be the most sensitive to our scenario, is the “ $SR3\ell - H$ ” signal region of Ref. [69], which looks for three leptons, no b -jets and large missing energy. This analysis considers 13 fb^{-1} of LHC data at $\sqrt{s} = 13 \text{ TeV}$. The integrated luminosity needed to exclude a particular value of the quadruplet mass at the 95 % C.L. can then be estimated as

$$\mathcal{L} = 13 \text{ fb}^{-1} \times \frac{1}{(s/s_{excl})^2}, \quad (2.30)$$

where s/s_{excl} is the number of expected signal events over the number of excluded signal events as reported by **CheckMate**. The corresponding result is represented by the thick solid line in the left bottom panel of Fig. 2. The thin solid line represents the luminosity required to test the different masses using the improved multi-lepton search described in Ref. [70]. As things stand, masses as large as $M \sim 600$ GeV can be tested in multi-lepton final states at the LHC. Getting ahead of the results discussed, we also show the reach of LHC Higgs-self couplings measurements as well as that of the gravitational wave observatory LISA; see right bottom panel in Fig. 2. Interestingly, the former cannot even test the parameter space region where the FOEWPT takes place. (As a matter of fact, in the present scenario the LHC Higgs-self couplings measurements are sensitive only to the region where the theory does not achieve EWSB.). These results suggest that most weakly-coupled models (those containing $SU(2)_L$ charged states), even if tuned to avoid large corrections to operators other than \mathcal{O}_6 , can be better tested at gravitational wave observatories or in direct LHC searches ¹¹.

2.5 Beyond the dimension-six effective field theory

Despite having shown that most scalar UV completions affecting only the Higgs potential at low energy require unnaturally large cancellations, a robust generic description of the EWPT in these scenarios is nonetheless worthwhile. This allows us to study the dynamics of the EWPT, including the reach of different facilities, once and for all. Any particular UV model would only need to be matched to the parameters of such description.

If new physics is heavy, as we are assuming in this work, an EFT description of the scalar potential is suggested. However, this can not only rely on operators of dimension six, given the small upper bound of f required by the SFOEWPT; see Eq. (2.18). Instead, dimension-eight deformations of the scalar potential have to be included, too, for the EFT to be more accurate. Moreover, dimension-eight operators appear naturally also in strongly-coupled theories. These are better described by means of the EW chiral Lagrangian ($ew\chi L$), subject to a different power counting as we detail below.

The $ew\chi L$ [71–83] is the most general EFT that describes the low-energy effects of strongly-coupled new physics. (Historically, it emerged from the Higgs-less chiral Lagrangian [84–87], which was then supplemented with a generic scalar singlet h .) Since this does not assume any IR-doublet structure for the Higgs, it describes a very wide class of new-physics models that induce large deviations in the Higgs sector from the SM. The leading-order $ew\chi L$

¹¹Note that most SM extensions avoiding large corrections to operators such as $\mathcal{O}_{\phi D}$ or \mathcal{O}_{d6} involve different multiplets and therefore charged (often doubly-charged) scalars. One possible counter-example is a singlet scalar whose own parameters are tuned; see Ref. [24].

is

$$\begin{aligned}
L_{\text{LO}}^{ew\chi} = & -\frac{1}{2}\langle G_{\mu\nu}G^{\mu\nu}\rangle - \frac{1}{2}\langle W_{\mu\nu}W^{\mu\nu}\rangle - \frac{1}{4}B_{\mu\nu}B^{\mu\nu} \\
& + i\bar{q}_L \not{D} q_L + i\bar{\ell}_L \not{D} \ell_L + i\bar{u}_R \not{D} u_R + i\bar{d}_R \not{D} d_R + i\bar{e}_R \not{D} e_R \\
& + \frac{v^2}{4} \text{Tr} (D_\mu U^\dagger D^\mu U) (1 + F(h)) + \frac{1}{2} \partial_\mu h \partial^\mu h - V(h) \\
& - \frac{v}{\sqrt{2}} \left[\bar{q}_L \left(Y_u + \sum_{n=1}^{\infty} Y_u^{(n)} \left(\frac{h}{v} \right)^n \right) U^{P_+ q_R} + \bar{q}_L \left(Y_d + \sum_{n=1}^{\infty} Y_d^{(n)} \left(\frac{h}{v} \right)^n \right) U^{P_- q_R} \right. \\
& \left. + \bar{\ell}_L \left(Y_e + \sum_{n=1}^{\infty} Y_e^{(n)} \left(\frac{h}{v} \right)^n \right) U^{P_- \ell_R} + \text{h.c.} \right], \tag{2.31}
\end{aligned}$$

where U stands for the exponential of the Goldstone matrix, G, W and B are the SM gauge fields, u_R, d_R, e_R, q_L and ℓ_L are the fermions of the SM, and Y are generalised Yukawa couplings. The scalar h couples through general polynomials to the other fields, which reflects its strongly-coupled origin.

These polynomials ($V(h)$, $F(h)$, and $Y_i(h) = Y_i + \sum_{n=1}^{\infty} Y_i^{(n)} (h/v)^n$) are not truncated at canonical dimension four, but go to arbitrary order. (An additional operator of the structure $(\partial_\mu h)(\partial^\mu h)f(h)$ is also allowed by symmetry, but can be removed via field redefinitions, without loss of generality [82].) The coefficients of these polynomials depend on v/f .

As the Lagrangian in Eq. (2.31) contains terms with arbitrarily high canonical dimension, the EFT can clearly not be organized in terms of canonical dimensions. Instead, it is organised by a generalisation of the momentum expansion of chiral perturbation theory [88], the chiral dimensions [82, 83]. They reflect an expansion in terms of loops, which guarantees the renormalizability of the EFT at a fixed order in the expansion. The cutoff of the EFT is at $\Lambda = 4\pi f$, yielding the expansion parameter $f^2/\Lambda^2 = 1/16\pi^2$. For $v < f$, the parameter $\xi = v^2/f^2$ is smaller than the unity and Eq. (2.31) can be further expanded in ξ . In this scenario, a double expansion in ξ and $1/16\pi^2$ organises the EFT [89], in the spirit of the strongly-interacting light Higgs Lagrangian [90].

In this double expansion, we still see some of the decoupling effects, but also a pattern of Wilson coefficients that is coming from the strong sector. Depending on the structure of the operators, they will be suppressed by ratios of scales (ξ , based on their canonical dimension) and loop factors ($1/16\pi^2$, based on their chiral dimension). This creates an additional hierarchy among the operators of a given canonical dimension, compared to the weakly-coupled case of section 2. Some of the dimension six operators, corresponding to $L_{\text{LO}}^{ew\chi}$, will only be suppressed by ξ , while other operators, corresponding to $L_{\text{NLO}}^{ew\chi}$, will be suppressed by an additional loop factor, resulting in $\xi/16\pi^2$. The former affects the Higgs sector with deviations of $\mathcal{O}(10\%)$, dominating over effects in the gauge-fermion sector of the latter group, with deviations of $\mathcal{O}(1\%)$ or below. This hierarchy also reflects the current experimental constraints: The gauge-fermion sector is rather strongly constrained, while large effects in the Higgs couplings are still possible. The $ew\chi L$ of Eq. (2.31) is now expanded in both chiral and canonical dimensions.

Since $\xi = \mathcal{O}(0.1-0.2)$ [32, 42, 63, 91], effects of $\mathcal{O}(\xi^2)$ could in principle be larger than the $\mathcal{O}(1/16\pi^2)$ effects. The leading effects in the double expansion are then given by expanding L_{LO} up to $\mathcal{O}(\xi^2)$. *A priori*, the Higgs potential, which at this order contains both \mathcal{O}_6 and \mathcal{O}_8 , is of chiral dimension 0 and the dominating effect. However, the Higgs mass is then expected to be of order $\mathcal{O}(\Lambda)$, which would break the EFT approach. In order for this to make sense, the Higgs mass must be parametrically suppressed to appear at chiral dimension of 2¹². An additional fine tuning of $\mathcal{O}(\xi)$ is needed for $m_h \sim v$. This, however, might only affect the mass term of the potential and the Higgs self-couplings could have large deviations from the SM, induced by c_6 and c_8 .

We can understand the enhancement on the operators in the potential by just dimensional analysis if we assume that the strongly-coupled theory is described by only one relevant coupling g_* . To this aim, we need to abandon the convention $\hbar = c = 1$ recovering the physical dimensions of these two constants. It turns out that the coefficient of any operator involving r Higgs insertions and q derivatives scales as $g_*^2 f^4 [h/f]^r [\partial/(g_* f)]^q$, up to $\mathcal{O}(1)$ coefficients [47, 90, 92, 93]. Hence, scalar operators not carrying derivatives are enhanced with respect to the derivative ones by several powers of g_* ($\gg 1$ in a strongly couple theory); *e.g.* $c_6 \sim g_*^2$ versus $c_{d6} \sim 1$. We refer to Ref. [94] for a discussion on which scenarios show this enhancement while still having $m_h \sim v$. We analyze the EWPT under this assumption in the next section. Thus, we restrict ourselves to the EFT including exclusively the operators \mathcal{O}_6 and \mathcal{O}_8 .

3 The electroweak phase transition

In this section we describe how to determine the VEV of the Higgs at the critical and nucleation temperatures, v_{T_c} and v_{T_n} , the latent heat of the phase transition, α , and the inverse duration time of the phase transition, β/H , in the non-minimal EFT. The results we obtain extend those previously obtained in the literature (see *e.g.* Refs. [19, 21]), where only \mathcal{O}_6 has been considered (despite the low cutoff and the consequent potential breaking of the EFT approach).

3.1 Finite temperature potential

The first ingredient we need is the Coleman-Weinberg effective potential at finite temperature; see Ref. [16] for a review. In the Landau gauge and in the \overline{MS} renormalization scheme, the one-loop effective potential $V_{1\ell}$ of our EFT scenario can be expressed as

$$V_{1\ell} = V_{\text{tree}} + \Delta V_{1\ell} , \quad (3.1)$$

¹²This occurs naturally in composite Higgs models (CHMs), where the Higgs potential is generated radiatively and then comes with two powers of weak couplings (g^2, y^2) and a corresponding loop suppression of the scale Λ^2 to the scale f^2 .

with

$$V_{\text{tree}} = -\frac{\mu^2}{2}h_c^2 + \frac{\lambda}{4}h_c^4 + \frac{c_6}{8f^2}h_c^6 + \frac{c_8}{16f^4}h_c^8, \quad (3.2)$$

$$\Delta V_{1\ell} = \Delta V_{1\ell,T=0} + V_{1\ell,T\neq 0}, \quad (3.3)$$

$$\Delta V_{1\ell,T=0} = \sum_{i=h,\chi,W,Z,t} \frac{n_i m_i^2(h_c)}{64\pi^2} \left(\log \frac{m_i^4(h_c)}{v^2} - C_i \right), \quad (3.4)$$

$$V_{1\ell,T\neq 0} = \frac{n_t T^4}{2\pi^2} J_f(m_t^2(h_c)/T^2) + \sum_{i=h,\chi,W,Z} \frac{n_i T^4}{2\pi^2} J_b(m_i^2(h_c)/T^2), \quad (3.5)$$

where $\Delta V_{1\ell,T=0}$ is the temperature-independent one-loop contribution and $V_{1\ell,T\neq 0}$ is the (one-loop) remaining part. The variable h_c is a constant background field of the Higgs. In Eq. (3.4), n_i are the degrees of freedom $n_W = 2n_Z = 2n_\chi = 6n_h = -n_t/2 = 6$, while C_i is equal to 5/6 for gauge bosons and 3/2 for scalars and fermions. The h_c -dependent squared masses m_i^2 are

$$m_h^2(h_c) = -\mu^2 + 3\lambda h_c^2 + \frac{15c_6}{4f^2}h_c^4 + \frac{7c_8}{2f^4}h_c^6, \quad (3.6)$$

$$m_\chi^2(h_c) = -\mu^2 + \lambda h_c^2 + \frac{3c_6}{4f^2}h_c^4 + \frac{c_8}{2f^4}h_c^6, \quad (3.7)$$

$$m_t^2(h_c) = \frac{h_t^2}{2}h_c^2, \quad m_W^2(h_c) = \frac{g^2}{4}h_c^2, \quad m_Z^2(h_c) = \frac{g^2 + g'^2}{4}h_c^2. \quad (3.8)$$

The explicit expression of the functions J_b and J_f , with or without the hard thermal loop resummation, can be found *e.g.* in Ref. [16, 95].

Since our main results turn out to be quite insensitive to details, we can set the Yukawa, $SU(2)_L$ and $U(1)_Y$ gauge couplings at tree level by fixing $m_t(v)$, $m_W(v)$ and $m_Z(v)$ in Eq. (3.8) at 172, 80 and 91 GeV, respectively. We moreover constrain μ^2 at tree level by requiring V_{tree} to have a minimum at $h_c = v$:

$$\mu^2 = \lambda v^2 + \frac{3c_6}{4f^2}v^4 + \frac{c_8}{2f^4}v^6. \quad (3.9)$$

Similarly, to set λ , we require $\partial^2 V(\phi_c)/\partial h_c^2|_{h_c=v} = (125 \text{ GeV})^2$, which implies

$$\lambda = -\frac{3c_6}{2f^2}v^2 - \frac{3c_8}{2f^4}v^4 + \frac{m_h^2}{2v^2}. \quad (3.10)$$

The remaining free parameters in $V_{1\ell}$ are therefore c_6/f^2 and c_8/f^4 . In section 4 we analyse the impact of the modified triple and quartic Higgs couplings

$$\lambda_3 = 1 + \frac{v^2}{m_h^2} \left(2c_6 \frac{v^2}{f^2} + 4c_8 \frac{v^4}{f^4} \right), \quad \lambda_4 = \frac{1}{4} + \frac{v^2}{m_h^2} \left(3c_6 \frac{v^2}{f^2} + 8c_8 \frac{v^4}{f^4} \right), \quad (3.11)$$

in current and future Higgs searches.

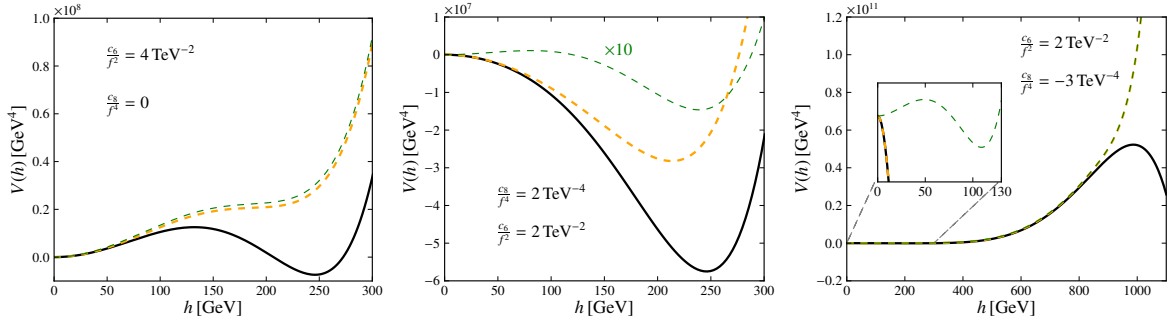


Figure 3. The potentials V_{tree} (black solid curve), $V_{1\ell}$ at $T = 0$ (orange dashed curve) and $V_{1\ell}$ at $T = T_x$ (green dashed curve) for the choices of c_6/f^2 and c_8/f^4 indicated in each panel. In the left panel, there exist two vacua already at zero temperature ($\mu^2 \simeq -3100 \text{ GeV}^2$, $\lambda \simeq -0.23$, $T_x = T_c = 35 \text{ GeV}$). In the central panel, the existence of two vacua arises only at finite temperature ($\mu^2 = 1900 \text{ GeV}^2$, $\lambda = -0.06$, $T_x = T_c = 82 \text{ GeV}$). In the right panel, the potential is unbounded from below, but the instability scale is above the cutoff $f = 1 \text{ TeV}$ ($\mu^2 = 3000 \text{ GeV}^2$, $\lambda = -0.03$, $T_x = T_n = 99 \text{ GeV}$). T_c is the critical temperature obtained in the mean-field approximation.

Notice that the EFT is a valid description of the theory only at energy scales much below f , therefore we do not address questions of the stability of the potential. Thus, we do not exclude *a priori* all values of c_8 and c_6 leading to $V_{1\ell}$ unbounded from below; we only require

$$V_{\text{tree}}(v) < V_{\text{tree}}(h_c) \quad \text{for any } h_c \in]v, f] . \quad (3.12)$$

This in practice corresponds to imposing a lower bound on c_8 that varies with f . Such constraint is $c_8 \gtrsim -9$ for $f = 1 \text{ TeV}$ and $c_8 \gtrsim -2$ for $f = 2 \text{ TeV}$. For concreteness, we limit the plots hereafter to the first bound.

Figure 3 shows the typical classes of potentials that we consider: Cases where the potential has a tree level barrier between the minima (left panel), cases where such a barrier is only due to a finite temperature (one-loop) effect (central panel), and cases where the potential is unbounded from below but the instability arises at a scale larger than f (right panel). See Ref. [96] for phenomenological discussions of new physics models in each class.

3.2 Mean-field estimates

From $V_{1\ell}$ it is straightforward to determine some quantities that roughly characterise the EWPT, namely T_c and v_{T_c}/T_c . The critical temperature, T_c , is the temperature at which the minima of the broken and unbroken phases are degenerate. It provides the upper bound on the temperature at which the EWPT really starts, T_n . The quantity v_{T_c}/T_c , with v_{T_c} being the VEV of the Higgs in the EW broken phase at $T = T_c$, is linked to the strength of the EWPT. Indeed, due to the fact that v_T/T typically decreases with increasing T , v_{T_c}/T_c can be used as a lower bound on the actual value of v_T/T during the EWPT (if the transition ever happens; see below).

The potential $V_{1\ell}$ is easy to treat numerically, but for analytic insights on T_c and v_{T_c}/T_c , the mean-field approximation may be helpful. We then begin neglecting $\Delta_{1\ell, T=0}V(h_c)$. In $\Delta_{1\ell, T \neq 0}V(h_c)$, we consider the high-temperature expansion of J_b and J_f and retain their leading terms, *i.e.* $J_b(x) \rightarrow \pi^2 x/12$ and $J_f(x) \rightarrow -\pi^2 x/24$ in Eq. (3.5). The potential $V_{1\ell}$ now reduces to the form

$$V_{\text{mean}}(\phi, T) = \frac{-\mu^2 + a_T T^2}{2} h_c^2 + \frac{\lambda}{4} h_c^4 + \frac{c_6}{8f^2} h_c^6 + \frac{c_8}{16f^4} h_c^8, \quad (3.13)$$

with $a_T = \frac{1}{16} \left(4 \frac{m_h^2}{v^2} + 3g^2 + g'^2 + 4y_t^2 - 12c_6 \frac{v^2}{f^2} - 12c_8 \frac{v^4}{f^4} \right)$.

In Eq. (3.13) the thermal contribution can only raise the potential at $h_c \neq 0$. No transition from the symmetric to the broken phase is conceivable if at zero temperature the EW breaking minimum is above the symmetric one. Hence, the condition $V_{\text{mean}}(v, T=0) < V_{\text{mean}}(0, T=0)$ has to be satisfied, which is equivalent to

$$\frac{c_6}{f^2} < \frac{m_h^2}{v^4} - \frac{3v^2}{2} \frac{c_8}{f^4}. \quad (3.14)$$

Saturating the inequality is not feasible. As previously mentioned, there must be a gap between T_c and T_n , and the stronger the phase transition is the larger is the gap. For this reason, values of c_6/f^2 close to the upper bound in Eq. (3.14) are not acceptable since they lead to $T_c \rightarrow 0$ and $v_{T_c}/T_c \rightarrow \infty$. In this limit the EWPT would never happen within the lifetime of the Universe. Such values of c_6/f^2 are thus expected to be ruled out by more sophisticated estimates; see section 3.3. For the same reason, it is at large c_6/f^2 that, whenever the EWPT can really start, the parameter scenarios with the strongest EWPTs arise. To appreciate the relevance of this effect, let us first evaluate the EWPT disregarding the issue.

We apply the analytic procedure of section 2.1 to the potential in Eq. (3.13). We fix the values of μ and λ as in Eqs. (3.9) and (3.10), and we require c_6 and c_8 to fulfil Eq. (3.12). Moreover, by definition, at $T = T_c$ the EWSB minimum is degenerate with the symmetric one. These properties lead to the following relations for v_{T_c} and T_c :

$$\begin{aligned} v_{T_c}^2 &= \left[-\frac{2c_6}{3c_8} \pm 2\sqrt{\frac{c_6^2}{9c_8^2} - \frac{\lambda}{3c_8}} \right] f^2, \\ T_c^2 &= \frac{\mu^2}{a_0} - \left[\frac{2c_6^3}{27c_8^2} - \frac{c_6\lambda}{3c_8} \mp 2\sqrt{\left(\frac{c_6^2}{9c_8} - \frac{\lambda}{3}\right)^3 \frac{1}{c_8}} \right] \frac{f^2}{a_0}, \end{aligned} \quad (3.15)$$

The left panel of Fig. 4 summarises our mean-field-approximation results in the plane $c_6/f^2 - c_8/f^4$. To the right of the whole shaded area, Eq. (3.14) is violated. Therefore, along the right border, $T_c = 0$ and $v_{T_c}/T_c = \infty$. On the left of it, the above conditions for a first order EWPT are not satisfied. Below it, instead, Eq. (3.12) is not satisfied for $f = 1$ TeV. (As previously explained, this border would move up or down by assuming different values of f .)

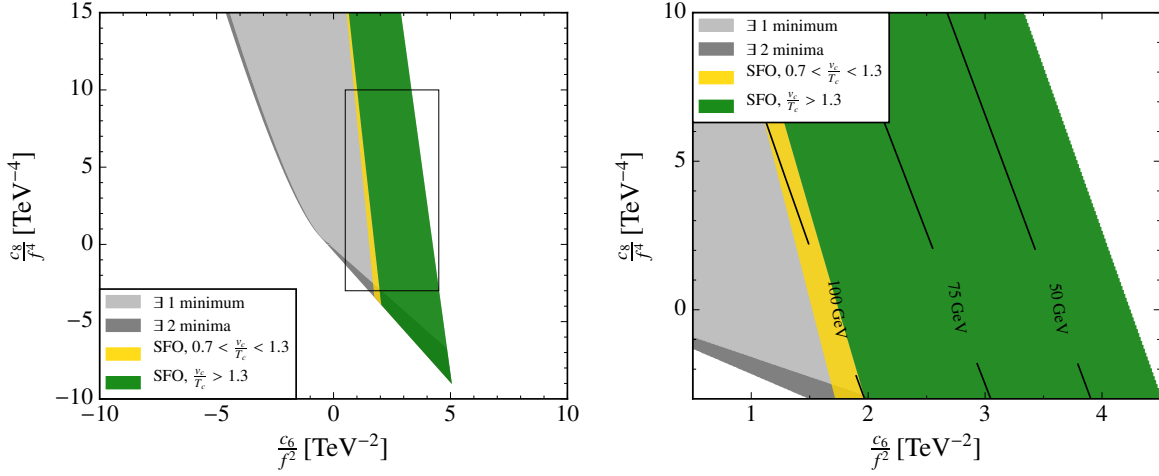


Figure 4. $c_6/f^2 - c_8/f^4$ plane of parameter space for a SFOEWPT in the mean-field approximation. Left) The filled region shows the allowed values for c_6 and c_8 such that at $T = 0$ the deepest minimum is at v . In the darker areas there is a second minimum above the one at v . For negative c_8 , we cut off the potential at 1 TeV and demand that $V(1\text{TeV}) > V(v)$ to ensure that the global minimum is at v . Superimposed are shades of yellow to green to show the strength of the phase transition, v_{T_c}/T_c , based on the critical temperature. Right) Zoomed version on the black rectangle of the left panel (note the different axis ranges). Lines of constant T_c are depicted.

The yellow and green regions mark the values of c_6/f^2 and c_8/f^2 leading to $0.7 < v_{T_c}/T_c < 1.3$ and $v_{T_c}/T_c > 1.3$, respectively. These regions are split into a darker and a lighter areas. For $c_8/f^2 < 0$ the former shows where V_{tree} is unbounded from below but the instability is above the cutoff (cf. right panel in Fig. 3); in the latter, V_{tree} does not provide any sign of instability below the cutoff (cf. left and central panels in Fig. 3). The same split is applied to the grey region where the EWPT is not strong. In the dark grey area with $c_8/f^2 > 0$, besides the global minimum at $h_c = v$, V_{tree} presents a further minimum at $h_c \in]v, f[$. We do not further discuss this peculiar configuration since it does not appear in the region with a SFOEWT. The right panel of Fig. 4 shows a zoom of the rectangle in the plot in the left panel. It also reports some contour curves for T_c .

3.3 Numerical procedure

The quantity v_{T_c}/T_c is a good estimate of the strength of the EWPT only when the gap between T_c and T_n is small. Quantitatively, T_n is defined as the temperature at which the probability for the nucleation of one single bubble (containing the broken phase) in a horizon volume is approximately ~ 1 . For our scenario, the nucleation temperature can be considered in practice as the temperature T_n such that $S_3[V_{1\ell}(h_c, T_n)] \simeq 140 T_n$, with S_3 the action of the thermal decay from the false to the true vacuum of $V_{1\ell}$ [16, 95]¹³. Analytically, S_3 can be

¹³This assumes the Universe to be dominated by radiation during the EWPT.

calculated in the limit of thin or thick wall bubbles [16], but in general we do not expect our bubble profiles to precisely fulfil any of these two limits. We thus determine S_3 numerically. For this scope, we use the code `CosmoTransition` [97] in which, to be more accurate, we do not implement the potential in the mean-field approximation but as in Eq. (3.1) with the hard-thermal loop resummations in J_b and J_f included ¹⁴.

The findings for T_n and v_{T_n}/T_n are respectively displayed in the top left and top right panels of Fig. 5 (dotted lines). As expected, for values of c_6/f^2 nearby its upper limit (right border of the gray area; cf. Eq. (3.14)), $S_3[V_{1\ell}(h_c, T)]/T$ is larger than 140 for any T , meaning that the EWPT never starts. This problem is avoided when $2c_6/f^2 + 3v^2c_8/f^4$ goes below the threshold of about 2.9 (black, thick dashed line). Conceptually, at the threshold one obtains $T_n = 0$ and $v_{T_n}/T_n = \infty$. The strongest EWPTs and largest supercoolings (namely, the gaps between T_n and T_c) are thus achieved just below this threshold. By departing from it (*i.e.* by reducing c_6/f^2 at fixed c_8/f^4), the supercooling is reduced and, in turn, v_{T_n}/T_n drops down. At some point, at about $2c_6/f^2 + 3v^2c_8/f^4 \approx 1.7$, the parameter v_{T_n}/T_n reaches 0.7, below which we do not draw any result. (We also omit the findings in the region where the EW vacuum instability is below the cutoff; see section 3.2.) The values of c_6/f^2 and c_8/f^4 relevant for the present paper are therefore those within the gray and yellow regions on the left of the dashed thick line.

The behaviour of T_n and T_c just described is also visible in the left panel of Fig. 6. As the figure highlights, for $v_{T_n}/T_n \gtrsim 4$ the discrepancy between T_n (evaluated with the full potential $V_{1\ell}$ and hard-thermal loop resummation) and T_c (evaluated in the mean-field approximation) is about 30%, whereas negligible for $v_{T_n}/T_n \lesssim 1$. From this point of view, what prevents the use of $v_{T_c}/T_c \gtrsim 1$ in the mean-field approximation as a bound for EW baryogenesis (instead of $v_{T_n}/T_n \gtrsim 1$) is not the accuracy of the result but the presence of a sizeable region where the nucleation never occurs. Interestingly, the nucleation requirement rules out the whole parameter region where there exists a tree-level barrier between the EW symmetric and EW broken vacua, as it happens when μ^2 and λ have the same signs (with the sign convention of Eq. (3.2)).

Within the allowed c_6/f^2 – c_8/f^4 parameter region, we also calculate the inverse duration time of the phase transition and the normalised latent heat. In our case we can approximate them, respectively, by $\beta/H = T_n \frac{d}{dT} \left(\frac{S_3}{T} \right)$ and $\alpha = \epsilon(T_n)/(35T_n^4)$, where $\epsilon(T_n)$ is the latent heat at the temperature T_n . We determine them by means of `CosmoTransition` ¹⁵. Their dependencies on c_6/f^2 and c_8/f^4 are presented in the bottom panels of Fig. 5. The correlation between T_n , v_{T_n}/T_n , α and β/H is evident. It is clear that all these quantities practically do not depend on c_6/f^2 and c_8/f^4 separately but only on $2c_6/f^2 + 3v^2c_8/f^4$. As expected, nearby the thick dashed line, where T_n is small and v_{T_n}/T_n is large, the EWPT exhibits small

¹⁴We also modified the code to evaluate the S_4 bubble action. Within the numerical precision of the code, we did not find significant changes, at least in the resolution relevant for our plots.

¹⁵In order to obtain β/H one has to modify the subroutine `transitionFinder.py`, as explained in Ref. [98]. Briefly, we determine β/H by first finding the temperature T_{240} at which $S_3[V_{1\ell}(h, T_{240})]/T_{240} = 240$, and then we use the approximation $\beta/H \simeq T_n(240 - 140)/(T_{240} - T_n)$.

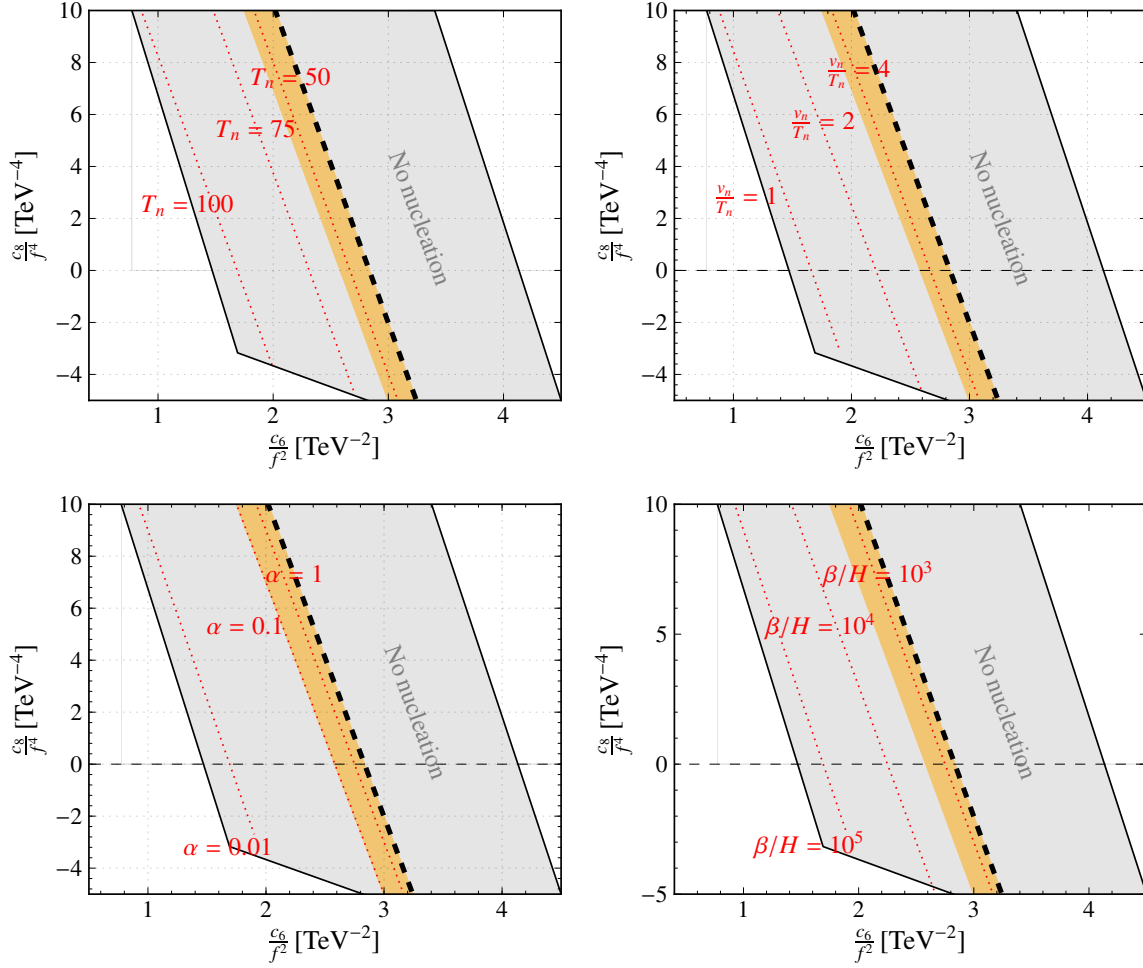


Figure 5. Values of T_n (top left), v_{T_n}/T_n (top right), α (bottom left) and β/H (bottom right) characterising the SFOEWPT in the plane c_6/f^2 – c_8/f^4 . The labels of T_n and T_c are in GeV units. On the right of the grey area the condition in Eq. (3.14) is violated. In the gray area to the right of the dashed line, the lifetime of the EW symmetric vacuum is longer than the age of the Universe, whereas on the left the transition results too weak for our purposes, i.e. $v_{T_n}/T_n < 0.7$. Below the grey area, the EW vacuum at zero temperature is not the global minimum at scales below the cutoff $f = 1$ TeV. In orange the parameter region LISA is sensitive to.

β/H and large α , typical of large supercoolings. The values of α and β/H that we obtain are more readable in Fig. 6 (right panel) where their values are expressed as a function of c_6/f^2 for $c_8/f^4 = 5 \text{ TeV}^{-4}$ (dotted curves), $c_8/f^4 = 2 \text{ TeV}^{-4}$ (dashed curves) and $c_8/f^4 = 0$ (solid curves). In general, for $c_8 = 0$, our results are in very good agreement with those of Ref. [19, 21].

A further quantity useful to characterise the EWPT is v_w , the velocity at which the

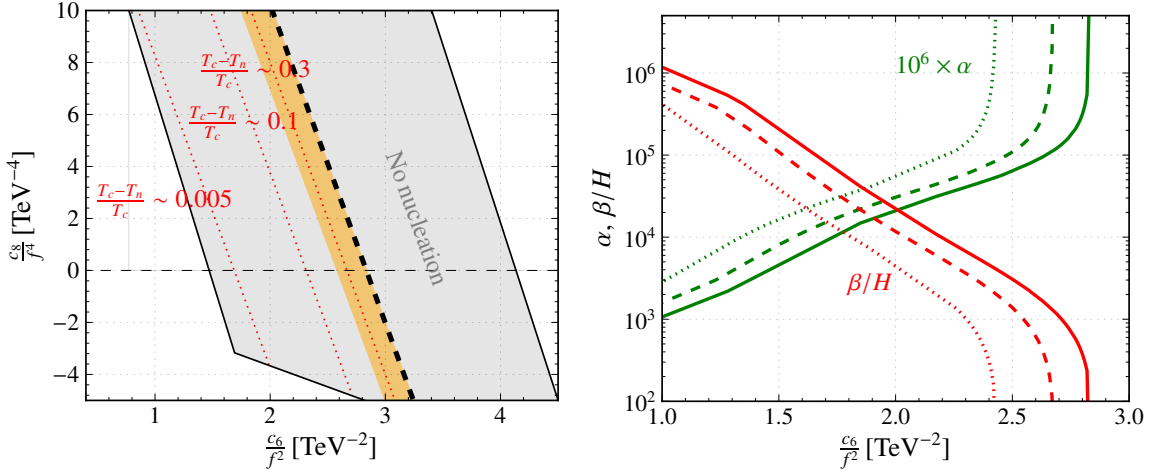


Figure 6. *Left panel)* The values of $(T_c - T_n)/T_c$ in the plane $c_6/f^2 - c_8/f^4$ (dotted lines). The rest stands as in Fig. 5. *Right panel)* The values of β/H and $10^6 \times \alpha$ as a function of c_6/f^2 for $c_8/f^4 = 5 \text{ TeV}^{-4}$ (dotted curves), $c_8/f^4 = 2 \text{ TeV}^{-4}$ (dashed curves) and $c_8/f^4 = 0$ (solid curves).

bubbles containing the broken phase expand into the EW symmetric phase. This speed results from the balance between the pressure difference between the two phases and the friction of the plasma on the bubbles. In general, the determination of v_w is subtle [20, 99–101]. Fortunately, for our aim, it is relevant to know v_w only when $v_{T_n}/T_n \gtrsim 4$; see below. In such a regime, on one side one expects $v \gtrsim 0.9$ [99], on the other v_w cannot reach the speed of light, even asymptotically [102, 103]. Due to this tiny window, it seems acceptable to take $v_w = 0.95$, for which we can straightforwardly adopt some results of the gravitational wave literature.

A SFOEWPT sources a gravitational wave stochastic background. Its power spectrum depends on v_w , T_n , β/H and α [104]. If the amplitude of the signal is strong enough, the LISA experiment will be able to detect it towards the end of the LHC [105]. Figure 4 in Ref. [104] shows the values of β/H and α that LISA can probe when $v_w \simeq 0.95$. We use this figure to forecast the capabilities of LISA for constraining the EFT we are working with¹⁶. The region that can be tested is marked in yellow in Figs. 5 and 6.

4 Interplay between gravitational wave signatures and Higgs-self coupling measurements

At low energy, the operators \mathcal{O}_6 and \mathcal{O}_8 modify the Higgs self couplings according to Eq. (3.11). These couplings have not been experimentally constrained yet. However, departures on the Higgs trilinear coupling beyond the range $[-0.7, 7.1]$ will be accessible at the 95% C.L. in the

¹⁶The LISA design approved by ESA has a sensitivity that is quite similar to that dubbed “C1” in Fig. 4 of Ref. [104]. For our analysis we then use the “C1” sensitivity region of that figure. Moreover, as *a posteriori* it turns out that LISA can probe our region when $T_n \lesssim 50 \text{ GeV}$, we use the result with $T_n = 50 \text{ GeV}$ of Ref. [104].

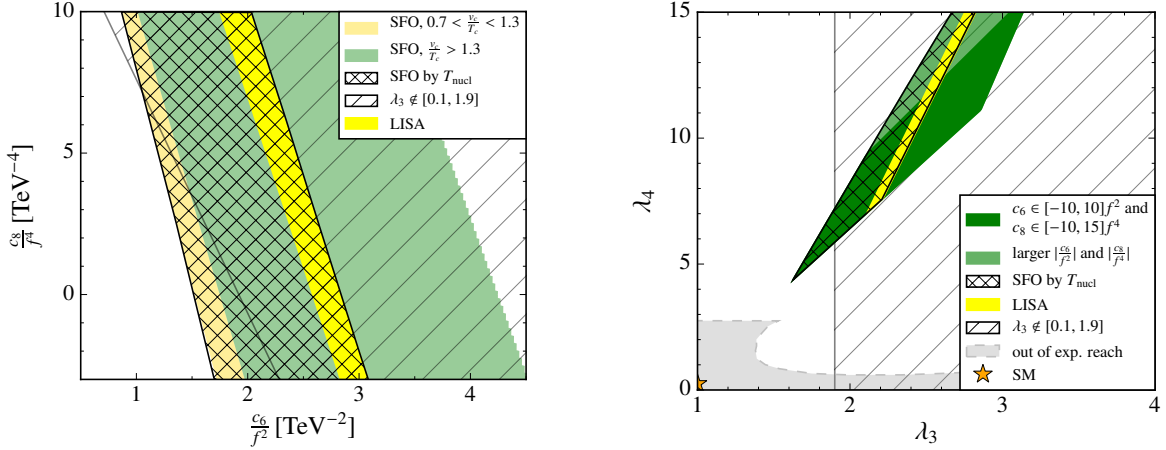


Figure 7. Left panel) Region of Fig. 4 where the SFOEWPT is achieved accordingly to the criterion $v_{T_n} \gtrsim T_n$ instead of $v_{T_c} \gtrsim T_c$. The reaches of FCC-ee [25] and LISA [104] are also displayed. Right panel) Allowed region translated to the λ_3 - λ_4 plane together with the future experimental sensitivities [27].

HL-LHC run [24–26]. Moreover, values outside the interval $[0.1, 1.9]$ [25] can be probed in a future FCC-ee facility [106]. Likewise, searches for double-Higgs and triple-Higgs production at future hadron colliders might also constrain λ_4 [27]. The reach of the different facilities is shown in the left panel of Fig. 7 as a function of $c_6/f^2, c_8/f^4$. In the right panel, this information is depicted in the plane λ_3 - λ_4 . The grey area in the latter shows the non-accessible region of a 100 TeV pp collider, taken from Ref. [27] (the reference cuts at $\lambda_4 = 2.75$, and so do we).

With LISA starting to take data in the early 2030’s, a sensible part of the parameter space where the SFOEWPT takes place would be first probed by LISA. Almost the complete parameter space would be tested at a future FCC-ee. A future hadron collider with 30 ab^{-1} [27] could be fully conclusive.

4.1 The effect of other potentially relevant operators

It might as well be the case that, differently from our assumption, new physics does not only affect the Higgs potential but generates other effects. As we outlined in section 2.5, the chiral Lagrangian describes new-physics setups in which the Higgs sector receives larger deviations from the SM than other sectors. This is the interesting scenario for a SFOEWPT. To account for all leading effects consistently, we therefore have to consider the full set of dimension-six and dimension-eight operators that contribute at chiral dimension 2 for the expansion in ξ .

The operators are

$$\begin{aligned} & \left(\phi^\dagger\phi\right)^3, \quad \partial_\mu\left(\phi^\dagger\phi\right)\partial^\mu\left(\phi^\dagger\phi\right), \quad \bar{\Psi}Y\phi\Psi\left(\phi^\dagger\phi\right), \\ & \left(\phi^\dagger\phi\right)^4, \quad \partial_\mu\left(\phi^\dagger\phi\right)\partial^\mu\left(\phi^\dagger\phi\right)\left(\phi^\dagger\phi\right), \quad \bar{\Psi}Y\phi\Psi\left(\phi^\dagger\phi\right)^2. \end{aligned} \quad (4.1)$$

With the identification $\phi = \frac{(v+h)}{\sqrt{2}} U_{(1)}^{(0)}$, we find at the different orders of ξ :

$$\begin{aligned} L_{\xi^0} &= \frac{1}{2}\partial_\mu h\partial^\mu h + \frac{\mu^2}{2}(v+h)^2 - \frac{\lambda}{4}(v+h)^4 - \frac{1}{\sqrt{2}}\bar{\Psi}\hat{Y}_\Psi UP_\pm\Psi(v+h) + \frac{v^2}{4}\text{Tr}(D_\mu U^\dagger D^\mu U)\left(1+\frac{h}{v}\right)^2, \\ L_{\xi^1} &= \frac{c_{d6}}{2f^2}\partial_\mu h\partial^\mu h(v+h)^2 - \frac{c_6}{8f^2}(v+h)^6 - \frac{1}{\sqrt{2}f^2}\bar{\Psi}\hat{Y}_\Psi^{(6)}UP_\pm\Psi(v+h)^3, \\ L_{\xi^2} &= \frac{c_{d8}}{2f^4}\partial_\mu h\partial^\mu h(v+h)^4 - \frac{c_8}{16f^4}(v+h)^8 - \frac{1}{\sqrt{2}f^4}\bar{\Psi}\hat{Y}_\Psi^{(8)}UP_\pm\Psi(v+h)^5. \end{aligned} \quad (4.2)$$

To bring the Lagrangian to the form of $L_{\text{LO}}^{ew\chi}$ in Eq. (2.31), we have to canonically normalise the field h using the field redefinition discussed in Ref. [82]. We find [107]

$$\begin{aligned} h \rightarrow h \Big\{ & 1 - \frac{\xi}{2}c_{d6}\left(1 + \frac{h}{v} + \frac{h^2}{3v^2}\right) + \xi^2 c_{d6}^2\left(\frac{3}{8} + \frac{h}{v} + \frac{13}{12}\left(\frac{h}{v}\right)^2 + \frac{13}{24}\left(\frac{h}{v}\right)^3 + \frac{13}{120}\left(\frac{h}{v}\right)^4\right) \\ & - \xi^2 c_{d8}\left(\frac{1}{2} + \frac{h}{v} + \left(\frac{h}{v}\right)^2 + \frac{1}{2}\left(\frac{h}{v}\right)^3 + \frac{1}{10}\left(\frac{h}{v}\right)^4\right) \Big\}. \end{aligned} \quad (4.3)$$

To first approximation, it coincides with Eq. (2.6). To obtain the right Higgs VEV and mass, the parameters μ^2 and λ have to fulfil

$$\begin{aligned} \mu^2 &= \frac{m_h^2}{2} + \frac{v^2}{f^2}\left(\frac{1}{2}c_{d6}m_h^2 - \frac{3}{4}c_6v^2\right) + \frac{v^4}{f^4}\left(\frac{1}{2}c_{d8}m_h^2 - c_8v^2\right), \\ \lambda &= \frac{m_h^2}{2v^2} + \frac{v^2}{f^2}\left(\frac{c_{d6}}{2}\frac{m_h^2}{v^2} - \frac{3c_6}{2}\right) + \frac{v^4}{f^4}\left(\frac{c_{d8}}{2}\frac{m_h^2}{v^2} - \frac{3c_8}{2}\right). \end{aligned} \quad (4.4)$$

Applying Eq. (4.3) everywhere in Eq. (4.2), we find the expansion of $V(h)$, $F(h)$, and $Y(h)$ in ξ . Writing

$$\begin{aligned} V(h) &= \frac{1}{2}m_h^2v^2\left[\frac{h^2}{v^2} + \sum_{i=3}^8\lambda_i\left(\frac{h}{v}\right)^i\right], \\ F(h) &= \sum_{i=1}^6f_i\left(\frac{h}{v}\right)^i, \end{aligned} \quad (4.5)$$

we finally have

$$\begin{aligned} \lambda_3 &= 1 + \frac{v^2}{f^2}\left(2c_6\frac{v^2}{m_h^2} - \frac{3}{2}c_{d6}\right) + \frac{v^4}{f^4}\left(\frac{15}{8}c_{d6}^2 - 3\frac{v^2}{m_h^2}c_6c_{d6} - \frac{5}{2}c_{d8} + 4\frac{v^2}{m_h^2}c_8\right), \\ \lambda_4 &= \frac{1}{4} + \frac{v^2}{f^2}\left(3c_6\frac{v^2}{m_h^2} - \frac{25}{12}c_{d6}\right) + \frac{v^4}{f^4}\left(\frac{11}{2}c_{d6}^2 - 9\frac{v^2}{m_h^2}c_6c_{d6} - \frac{21}{4}c_{d8} + 8\frac{v^2}{m_h^2}c_8\right), \end{aligned} \quad (4.6)$$

$$\begin{aligned}
f_1 &= 2 - \frac{v^2}{f^2} c_{d6} + \frac{v^4}{f^4} \left(\frac{3}{4} c_{d6}^2 - c_{d8} \right), \\
f_2 &= 1 - 2 \frac{v^2}{f^2} c_{d6} + \frac{v^4}{f^4} (3c_{d6}^2 - 3c_{d8})
\end{aligned} \tag{4.7}$$

and

$$\begin{aligned}
Y_\Psi^{(1)} &= Y_\Psi + \frac{v^2}{f^2} \left(2\hat{Y}_\Psi^{(6)} - \frac{c_{d6}}{2} Y_\Psi \right) + \frac{v^4}{f^4} \left(4\hat{Y}_\Psi^{(8)} - \frac{c_{d8}}{2} Y_\Psi - c_{d6} \hat{Y}_\Psi^{(6)} + \frac{3}{8} c_{d6}^2 Y_\Psi \right), \\
Y_\Psi^{(2)} &= \frac{v^2}{f^2} \left(3\hat{Y}_\Psi^{(6)} - \frac{c_{d6}}{2} Y_\Psi \right) + \frac{v^4}{f^4} \left(10\hat{Y}_\Psi^{(8)} - c_{d8} Y_\Psi - 4c_{d6} \hat{Y}_\Psi^{(6)} + c_{d6}^2 Y_\Psi \right),
\end{aligned} \tag{4.8}$$

where we only list the couplings relevant for the subsequent discussion. The matrices Y_Ψ and $Y_\Psi^{(n)}$ are the fermion mass and Yukawa matrices defined in Eq. (2.31). Note that the functional dependence of Eqs. (4.6) and (4.8) on c_i differ from the result of Refs. [89, 107], as we do not include explicit factors of λ in the definition of the Wilson coefficients. Already now we see two of the implications of adding these effective operators. The triple- and quartic-Higgs couplings are further modified with respect to the SM. Moreover, new vertices, such as $\bar{\Psi}\Psi hh$, also relevant for the study of double-Higgs production, arise.

Additionally, for current Higgs observables, also the local GGh and $\gamma\gamma h$ operators are important, even though they are formally of next-to-leading order. This is because these amplitudes arise at the one-loop level of the leading-order Lagrangian; see Ref. [108]. Such a Lagrangian is

$$L_{GGh} = L_{kin} + G_{\mu\nu} G^{\mu\nu} \left[\frac{c_{g6}}{16\pi^2 f^2} \phi^\dagger \phi + \frac{c_{g8}}{16\pi^2 f^4} (\phi^\dagger \phi)^2 \right]. \tag{4.9}$$

After symmetry breaking and the field redefinition of Eq. (4.3), this creates a contribution that renormalizes the gluon kinetic term and therefore $G_{\mu\nu}$. After this renormalization, we find

$$L_{GGh} = G_{\mu\nu} G^{\mu\nu} \left[1 + f_{G1} \frac{h}{v} + f_{G2} \frac{h^2}{v^2} + \mathcal{O}(h^3) \right], \tag{4.10}$$

with

$$\begin{aligned}
16\pi^2 f_{G1} &= \xi c_{g6} + \xi^2 \left(c_{g8} - \frac{1}{2} c_{d6} c_{g6} - \frac{c_{g6}^2}{32\pi^2} \right), \\
32\pi^2 f_{G2} &= \xi c_{g6} + \xi^2 \left(3c_{g8} - \frac{1}{2} c_{d6} c_{g6} - \frac{c_{g6}^2}{32\pi^2} \right).
\end{aligned} \tag{4.11}$$

The last term in each of the f_{Gi} comes from the renormalization and is sub-leading. Finally, it is also worth noting that all these operators would contribute to the EWPT, as they alter the h_c -dependent squared masses m_i^2 in Eqs. (3.6)-(3.8). In addition, the derivative operator \mathcal{O}_{d6} requires a reevaluation of the Coleman-Weinberg effective potential at finite temperature, as the field redefinition of Eq. (4.3) cannot be done in the unbroken phase [109, 110]. All these effects would be suppressed by v^2/f^2 in a_0 , but would nevertheless have an impact on the computation of the quantities of the EWPT.

Current experimental results only constrain effective couplings with a single Higgs field [32, 42], namely $Y_{t,b,\tau}^{(1)}$, f_1 , and f_{G1} from the list above. From these, f_1 is the most constrained, but still allows for deviations of $\mathcal{O}(5\%)$. The others are not constrained beyond $\mathcal{O}(10\%)$. While from a bottom-up point of view a deviation in one of these couplings might hint to a deviation in λ_3 of comparable size, such conclusions are strongly model dependent.

Double Higgs production, which would shed light on the λ_3 coupling of the Higgs potential in the SM, depends on five of the effective parameters from above [26, 111] if we restrict ourselves to the top loops only. These are $Y_t^{(1)}$, $Y_t^{(2)}$, f_{G1} , f_{G2} , and λ_3 . A large deviation in λ_3 from its SM value could then be not seen in the experiment because of the interplay with the otherwise unconstrained other parameters.

5 Conclusions

It is well known that the presence of higher-dimensional operators in the Standard Model Higgs potential can drastically influence the dynamics of the ElectroWeak (EW) symmetry breaking. Among the possible operators, the interactions $\mathcal{O}_n = (\phi^\dagger \phi)^{\frac{n}{2}}$, with ϕ being the Higgs doublet, have attracted a lot of attention to make the EW Phase Transition (EWPT) strongly first order while evading any scheduled LHC search. Collider searches sensitive to these operators are only feasible in future facilities like the ILC or the FCC, which can measure the rate of double and (to a lesser extent) triple Higgs productions accurately. Thus, in the LHC era, it will be difficult to prove the existence of new heavy physics compatible with the Strong First-Order EWPT (SFOEWPT) *if* the EW-scale description of the UltraViolet (UV) theory exhibits *only* the operators \mathcal{O}_n . In the present paper we have discussed whether such a thread is plausible.

First, we have scrutinised whether UV theories can be described, in the infrared, by an Effective Field Theory (EFT) where \mathcal{O}_6 is the only non-negligible higher-dimensional operator, and lead to a SFOEWPT. We have found that, in general, the suppression of all the other dimension-six operators is problematic. We have indeed proven that in weakly-coupled setups consisting of new scalars:

- Whenever \mathcal{O}_6 is generated by heavy singlets and/or triplets, there must exist other dimension-six operators with signatures that can be detected by the end of the HL-LHC run;
- If doublets are inducing \mathcal{O}_6 , numerous dimension-six operators need to be suppressed by hand;
- If \mathcal{O}_6 is sourced by a generic higher-representation multiplet, there is tension with the EW ρ parameter. In this case, the new physics scale is often light enough to appear in future LHC multi-lepton searches, too;

- Caveats however exist. For instance heavy quadruplets producing \mathcal{O}_6 can be embedded in a custodial setup that naturally overcomes the EW precision tests.

Of course, in a weakly-coupled scenario with several scalars, a tuning in the fundamental parameters can still yield to an EFT where the coefficient of \mathcal{O}_6 is substantially larger than those of the other dimension-six operators. However, even this SFOEWPT scenario is expected not to be correctly described at low energies by means of a dimension-six EFT. Achieving a SFOEWPT indeed requires $c_6/f^2 \gtrsim 1 \text{ TeV}^{-2}$, with f the cutoff of the theory. This implies that f is likely too close to the EW scale for the dimension-six EFT to be valid, at least in weakly-coupled theories. Dimension-eight operators have to be thus considered, which is also the case when strongly-coupled sectors are present. Such sectors can also lead to naturally large corrections to the Higgs potential (in comparison with other operators). In view of this possibility, we have also examined the EFT where (only) both \mathcal{O}_6 and \mathcal{O}_8 are unsuppressed.

In the aforementioned dimension-eight setup, we have computed for the first time the parameters relevant for the EWPT, including the critical and nucleation temperatures and the VEVs of the Higgs at these temperatures. We have also estimated the latent heat and the inverse duration time of the phase transition, characterising the gravitational waves produced in the collisions of nucleated bubbles. Regarding the coefficients of \mathcal{O}_6 and \mathcal{O}_8 , c_6 and c_8 respectively, we have obtained that the parameter region $2.5 \lesssim c_6/f^2 + 3v^2c_8/(2f^4) \lesssim 2.9$ is in the reach of the future LISA experiment. Remarkably, due to the low LHC sensitivity to \mathcal{O}_6 and \mathcal{O}_8 , LISA will be the first experiment able to significantly constrain these operators.

Finally, we have commented on the reach of future colliders. We have shown that almost all values of interest will be probed by a future FCC-ee in double-Higgs production, while the whole parameter space will be testable combining double- and triple-Higgs production in hadronic colliders.

Acknowledgments

We are grateful to Florian Staub for useful support on SARAH. MC acknowledges AEC for hospitality during the first state of this project. CK thanks Andrew J. Long for discussions about the effective potential, and the Enrico Fermi Institute at the University of Chicago and Fermi National Laboratory for hospitality, where parts of this research was carried out. CK acknowledges also fruitful discussions at the LHCPHENO 2017 workshop at IFIC Valencia. MC is supported by the Royal Society under the the Newton International Fellowships program. The work of CK is supported in part by the Spanish Government and ERDF funds from the EU Commission [Grants No. FPA2014-53631-C2-1-P and SEV-2014-0398]. GN is financed by the Swiss National Science Foundation (SNF) under grant 200020-168988.

References

- [1] V. A. Kuzmin, V. A. Rubakov and M. E. Shaposhnikov, *On the Anomalous Electroweak Baryon Number Nonconservation in the Early Universe*, *Phys. Lett.* **155B** (1985) 36.

- [2] K. Kajantie, M. Laine, K. Rummukainen and M. E. Shaposhnikov, *Is there a hot electroweak phase transition at $m(H)$ larger or equal to $m(W)$?*, *Phys. Rev. Lett.* **77** (1996) 2887–2890, [[hep-ph/9605288](#)].
- [3] K. Rummukainen, M. Tsypin, K. Kajantie, M. Laine and M. E. Shaposhnikov, *The Universality class of the electroweak theory*, *Nucl. Phys.* **B532** (1998) 283–314, [[hep-lat/9805013](#)].
- [4] M. Laine and K. Rummukainen, *What’s new with the electroweak phase transition?*, *Nucl. Phys. Proc. Suppl.* **73** (1999) 180–185, [[hep-lat/9809045](#)].
- [5] F. Csikor, Z. Fodor and J. Heitger, *Endpoint of the hot electroweak phase transition*, *Phys. Rev. Lett.* **82** (1999) 21–24, [[hep-ph/9809291](#)].
- [6] P. Creminelli, A. Nicolis and R. Rattazzi, *Holography and the electroweak phase transition*, *JHEP* **03** (2002) 051, [[hep-th/0107141](#)].
- [7] L. Randall and G. Servant, *Gravitational waves from warped spacetime*, *JHEP* **05** (2007) 054, [[hep-ph/0607158](#)].
- [8] G. Nardini, M. Quiros and A. Wulzer, *A Confining Strong First-Order Electroweak Phase Transition*, *JHEP* **09** (2007) 077, [[0706.3388](#)].
- [9] T. Konstandin, G. Nardini and M. Quiros, *Gravitational Backreaction Effects on the Holographic Phase Transition*, *Phys. Rev.* **D82** (2010) 083513, [[1007.1468](#)].
- [10] J. Garcia-Bellido, D. Yu. Grigoriev, A. Kusenko and M. E. Shaposhnikov, *Nonequilibrium electroweak baryogenesis from preheating after inflation*, *Phys. Rev.* **D60** (1999) 123504, [[hep-ph/9902449](#)].
- [11] L. M. Krauss and M. Trodden, *Baryogenesis below the electroweak scale*, *Phys. Rev. Lett.* **83** (1999) 1502–1505, [[hep-ph/9902420](#)].
- [12] J. Garcia-Bellido, M. Garcia Perez and A. Gonzalez-Arroyo, *Symmetry breaking and false vacuum decay after hybrid inflation*, *Phys. Rev.* **D67** (2003) 103501, [[hep-ph/0208228](#)].
- [13] J. Smit and A. Tranberg, *Chern-Simons number asymmetry from CP violation at electroweak tachyonic preheating*, *JHEP* **12** (2002) 020, [[hep-ph/0211243](#)].
- [14] T. Konstandin and G. Servant, *Natural Cold Baryogenesis from Strongly Interacting Electroweak Symmetry Breaking*, *JCAP* **1107** (2011) 024, [[1104.4793](#)].
- [15] B. von Harling and G. Servant, *QCD-induced Electroweak Phase Transition*, *JHEP* **01** (2018) 159, [[1711.11554](#)].
- [16] M. Quiros, *Finite temperature field theory and phase transitions*, in *Proceedings, Summer School in High-energy physics and cosmology: Trieste, Italy, June 29-July 17, 1998*, pp. 187–259, 1999. [[hep-ph/9901312](#)].
- [17] D. E. Morrissey and M. J. Ramsey-Musolf, *Electroweak baryogenesis*, *New J. Phys.* **14** (2012) 125003, [[1206.2942](#)].
- [18] X.-m. Zhang, *Operators analysis for Higgs potential and cosmological bound on Higgs mass*, *Phys. Rev.* **D47** (1993) 3065–3067, [[hep-ph/9301277](#)].
- [19] C. Grojean, G. Servant and J. D. Wells, *First-order electroweak phase transition in the standard model with a low cutoff*, *Phys. Rev.* **D71** (2005) 036001, [[hep-ph/0407019](#)].

- [20] D. Bodeker, L. Fromme, S. J. Huber and M. Seniuch, *The Baryon asymmetry in the standard model with a low cut-off*, *JHEP* **02** (2005) 026, [[hep-ph/0412366](#)].
- [21] C. Delaunay, C. Grojean and J. D. Wells, *Dynamics of Non-renormalizable Electroweak Symmetry Breaking*, *JHEP* **04** (2008) 029, [[0711.2511](#)].
- [22] B. Grinstein and M. Trott, *Electroweak Baryogenesis with a Pseudo-Goldstone Higgs*, *Phys. Rev.* **D78** (2008) 075022, [[0806.1971](#)].
- [23] P. H. Damgaard, A. Haarr, D. O’Connell and A. Tranberg, *Effective Field Theory and Electroweak Baryogenesis in the Singlet-Extended Standard Model*, *JHEP* **02** (2016) 107, [[1512.01963](#)].
- [24] S. Di Vita, C. Grojean, G. Panico, M. Riembau and T. Vantalón, *A global view on the Higgs self-coupling*, [1704.01953](#).
- [25] S. Di Vita, G. Durieux, C. Grojean, J. Gu, Z. Liu, G. Panico et al., *A global view on the Higgs self-coupling at lepton colliders*, [1711.03978](#).
- [26] J. H. Kim, Y. Sakaki and M. Son, *Combined analysis of double Higgs production via gluon fusion at the HL-LHC in the effective field theory approach*, [1801.06093](#).
- [27] A. Papaefstathiou and K. Sakurai, *Triple Higgs boson production at a 100 TeV proton-proton collider*, *JHEP* **02** (2016) 006, [[1508.06524](#)].
- [28] B. Grzadkowski, M. Iskrzynski, M. Misiak and J. Rosiek, *Dimension-Six Terms in the Standard Model Lagrangian*, *JHEP* **10** (2010) 085, [[1008.4884](#)].
- [29] J. de Blas, M. Chala, M. Perez-Victoria and J. Santiago, *Observable Effects of General New Scalar Particles*, *JHEP* **04** (2015) 078, [[1412.8480](#)].
- [30] Y. Jiang and M. Trott, *On the non-minimal character of the SMEFT*, *Phys. Lett.* **B770** (2017) 108–116, [[1612.02040](#)].
- [31] J. de Blas, J. C. Criado, M. Perez-Victoria and J. Santiago, *Effective description of general extensions of the Standard Model: the complete tree-level dictionary*, [1711.10391](#).
- [32] J. de Blas, O. Eberhardt and C. Krause, *Current and future constraints on Higgs couplings in the electroweak chiral Lagrangian*, In preparation, .
- [33] P. Huang, A. Joglekar, B. Li and C. E. M. Wagner, *Probing the Electroweak Phase Transition at the LHC*, *Phys. Rev.* **D93** (2016) 055049, [[1512.00068](#)].
- [34] A. Riotto, *Theories of baryogenesis*, in *Proceedings, Summer School in High-energy physics and cosmology: Trieste, Italy, June 29-July 17, 1998*, pp. 326–436, 1998. [hep-ph/9807454](#).
- [35] D. Comelli, D. Grasso, M. Pietroni and A. Riotto, *The Sphaleron in a magnetic field and electroweak baryogenesis*, *Phys. Lett.* **B458** (1999) 304–309, [[hep-ph/9903227](#)].
- [36] A. De Simone, G. Nardini, M. Quiros and A. Riotto, *Magnetic Fields at First Order Phase Transition: A Threat to Electroweak Baryogenesis*, *JCAP* **1110** (2011) 030, [[1107.4317](#)].
- [37] H. H. Patel and M. J. Ramsey-Musolf, *Baryon Washout, Electroweak Phase Transition, and Perturbation Theory*, *JHEP* **07** (2011) 029, [[1101.4665](#)].
- [38] M. Garny and T. Konstandin, *On the gauge dependence of vacuum transitions at finite temperature*, *JHEP* **07** (2012) 189, [[1205.3392](#)].

- [39] X. Gan, A. J. Long and L.-T. Wang, *Electroweak sphaleron with dimension-six operators*, *Phys. Rev.* **D96** (2017) 115018, [[1708.03061](#)].
- [40] M. Carena, G. Nardini, M. Quiros and C. E. M. Wagner, *The Effective Theory of the Light Stop Scenario*, *JHEP* **10** (2008) 062, [[0806.4297](#)].
- [41] M. Carena, G. Nardini, M. Quiros and C. E. M. Wagner, *The Baryogenesis Window in the MSSM*, *Nucl. Phys.* **B812** (2009) 243–263, [[0809.3760](#)].
- [42] G. Buchalla, O. Cata, A. Celis and C. Krause, *Fitting Higgs Data with Nonlinear Effective Theory*, *Eur. Phys. J.* **C76** (2016) 233, [[1511.00988](#)].
- [43] R. Alonso, E. E. Jenkins, A. V. Manohar and M. Trott, *Renormalization Group Evolution of the Standard Model Dimension Six Operators III: Gauge Coupling Dependence and Phenomenology*, *JHEP* **04** (2014) 159, [[1312.2014](#)].
- [44] J. de Blas, *Electroweak limits on physics beyond the Standard Model*, *EPJ Web Conf.* **60** (2013) 19008, [[1307.6173](#)].
- [45] Q.-H. Cao, F. P. Huang, K.-P. Xie and X. Zhang, *Testing the electroweak phase transition in scalar extension models at lepton colliders*, [1708.04737](#).
- [46] L. Di Luzio, R. Grber and M. Spannowsky, *Maxi-sizing the trilinear Higgs self-coupling: how large could it be?*, [1704.02311](#).
- [47] M. Chala, G. Durieux, C. Grojean, L. de Lima and O. Matsedonskyi, *Minimally extended SILH*, [1703.10624](#).
- [48] L. Vecchi, *A dangerous irrelevant UV-completion of the composite Higgs*, *JHEP* **02** (2017) 094, [[1506.00623](#)].
- [49] G. Ferretti and D. Karateev, *Fermionic UV completions of Composite Higgs models*, *JHEP* **03** (2014) 077, [[1312.5330](#)].
- [50] H. Georgi and M. Machacek, *DOUBLY CHARGED HIGGS BOSONS*, *Nucl. Phys.* **B262** (1985) 463–477.
- [51] R. Slansky, *Group Theory for Unified Model Building*, *Phys. Rept.* **79** (1981) 1–128.
- [52] R. Feger and T. W. Kephart, *LieARTA Mathematica application for Lie algebras and representation theory*, *Comput. Phys. Commun.* **192** (2015) 166–195, [[1206.6379](#)].
- [53] E. Witten, *Mass Hierarchies in Supersymmetric Theories*, *Phys. Lett.* **105B** (1981) 267.
- [54] G. R. Dvali, *Why is the Higgs doublet light?*, *Phys. Lett.* **B324** (1994) 59–65.
- [55] H. Georgi, *AN ALMOST REALISTIC GAUGE HIERARCHY*, *Phys. Lett.* **108B** (1982) 283–284.
- [56] A. Masiero, D. V. Nanopoulos, K. Tamvakis and T. Yanagida, *Naturally Massless Higgs Doublets in Supersymmetric SU(5)*, *Phys. Lett.* **115B** (1982) 380–384.
- [57] K. S. Babu, I. Gogoladze and Z. Tavartkiladze, *Missing Partner Mechanism in SO(10) Grand Unification*, *Phys. Lett.* **B650** (2007) 49–56, [[hep-ph/0612315](#)].
- [58] K. S. Babu and S. M. Barr, *Natural suppression of Higgsino mediated proton decay in supersymmetric SO(10)*, *Phys. Rev.* **D48** (1993) 5354–5364, [[hep-ph/9306242](#)].

- [59] T. Hambye, F. S. Ling, L. Lopez Honorez and J. Rocher, *Scalar Multiplet Dark Matter*, *JHEP* **07** (2009) 090, [[0903.4010](#)].
- [60] K. S. Babu, S. Nandi and Z. Tavartkiladze, *New Mechanism for Neutrino Mass Generation and Triply Charged Higgs Bosons at the LHC*, *Phys. Rev.* **D80** (2009) 071702, [[0905.2710](#)].
- [61] K. Ghosh, S. Jana and S. Nandi, *Neutrino Mass Generation and 750 GeV Diphoton excess via photon-photon fusion at the Large Hadron Collider*, [1607.01910](#).
- [62] PARTICLE DATA GROUP collaboration, C. Patrignani et al., *Review of Particle Physics*, *Chin. Phys.* **C40** (2016) 100001.
- [63] ATLAS, CMS collaboration, G. Aad et al., *Measurements of the Higgs boson production and decay rates and constraints on its couplings from a combined ATLAS and CMS analysis of the LHC pp collision data at $\sqrt{s} = 7$ and 8 TeV*, *JHEP* **08** (2016) 045, [[1606.02266](#)].
- [64] F. Staub, *SARAH 4 : A tool for (not only SUSY) model builders*, *Comput. Phys. Commun.* **185** (2014) 1773–1790, [[1309.7223](#)].
- [65] J. Alwall, R. Frederix, S. Frixione, V. Hirschi, F. Maltoni, O. Mattelaer et al., *The automated computation of tree-level and next-to-leading order differential cross sections, and their matching to parton shower simulations*, *JHEP* **07** (2014) 079, [[1405.0301](#)].
- [66] A. Alloul, N. D. Christensen, C. Degrande, C. Duhr and B. Fuks, *FeynRules 2.0 - A complete toolbox for tree-level phenomenology*, *Comput. Phys. Commun.* **185** (2014) 2250–2300, [[1310.1921](#)].
- [67] T. Sjostrand, S. Mrenna and P. Z. Skands, *PYTHIA 6.4 Physics and Manual*, *JHEP* **05** (2006) 026, [[hep-ph/0603175](#)].
- [68] D. Dercks, N. Desai, J. S. Kim, K. Rolbiecki, J. Tattersall and T. Weber, *CheckMATE 2: From the model to the limit*, *Comput. Phys. Commun.* **221** (2017) 383–418, [[1611.09856](#)].
- [69] ATLAS COLLABORATION collaboration, *Search for supersymmetry with two and three leptons and missing transverse momentum in the final state at $\sqrt{s} = 13$ TeV with the ATLAS detector*, Tech. Rep. ATLAS-CONF-2016-096, CERN, Geneva, Sep, 2016.
- [70] J. Alcaide, M. Chala and A. Santamaria, *LHC signals of radiatively-induced neutrino masses and implications for the Zee-Babu model*, [1710.05885](#).
- [71] F. Feruglio, *The Chiral approach to the electroweak interactions*, *Int. J. Mod. Phys.* **A8** (1993) 4937–4972, [[hep-ph/9301281](#)].
- [72] J. Bagger, V. D. Barger, K.-m. Cheung, J. F. Gunion, T. Han, G. A. Ladinsky et al., *The Strongly interacting W W system: Gold plated modes*, *Phys. Rev.* **D49** (1994) 1246–1264, [[hep-ph/9306256](#)].
- [73] V. Koulovassilopoulos and R. S. Chivukula, *The Phenomenology of a nonstandard Higgs boson in $W(L) W(L)$ scattering*, *Phys. Rev.* **D50** (1994) 3218–3234, [[hep-ph/9312317](#)].
- [74] C. P. Burgess, J. Matias and M. Pospelov, *A Higgs or not a Higgs? What to do if you discover a new scalar particle*, *Int. J. Mod. Phys.* **A17** (2002) 1841–1918, [[hep-ph/9912459](#)].
- [75] L.-M. Wang and Q. Wang, *Electroweak chiral Lagrangian for neutral Higgs boson*, *Chin. Phys. Lett.* **25** (2008) 1984, [[hep-ph/0605104](#)].

- [76] B. Grinstein and M. Trott, *A Higgs-Higgs bound state due to new physics at a TeV*, *Phys. Rev. D* **76** (2007) 073002, [[0704.1505](#)].
- [77] R. Contino, C. Grojean, M. Moretti, F. Piccinini and R. Rattazzi, *Strong Double Higgs Production at the LHC*, *JHEP* **05** (2010) 089, [[1002.1011](#)].
- [78] R. Contino, *The Higgs as a Composite Nambu-Goldstone Boson*, in *Physics of the large and the small, TASI 09, proceedings of the Theoretical Advanced Study Institute in Elementary Particle Physics, Boulder, Colorado, USA, 1-26 June 2009*, pp. 235–306, 2011. [1005.4269](#). DOI.
- [79] A. Azatov, R. Contino and J. Galloway, *Model-Independent Bounds on a Light Higgs*, *JHEP* **04** (2012) 127, [[1202.3415](#)].
- [80] R. Alonso, M. B. Gavela, L. Merlo, S. Rigolin and J. Yepes, *The Effective Chiral Lagrangian for a Light Dynamical "Higgs Particle"*, *Phys. Lett. B* **722** (2013) 330–335, [[1212.3305](#)].
- [81] G. Buchalla and O. Cata, *Effective Theory of a Dynamically Broken Electroweak Standard Model at NLO*, *JHEP* **07** (2012) 101, [[1203.6510](#)].
- [82] G. Buchalla, O. Catà and C. Krause, *Complete Electroweak Chiral Lagrangian with a Light Higgs at NLO*, *Nucl. Phys. B* **880** (2014) 552–573, [[1307.5017](#)].
- [83] G. Buchalla, O. Catà and C. Krause, *On the Power Counting in Effective Field Theories*, *Phys. Lett. B* **731** (2014) 80–86, [[1312.5624](#)].
- [84] T. Appelquist and C. W. Bernard, *Strongly Interacting Higgs Bosons*, *Phys. Rev. D* **22** (1980) 200.
- [85] A. C. Longhitano, *Low-Energy Impact of a Heavy Higgs Boson Sector*, *Nucl. Phys. B* **188** (1981) 118–154.
- [86] A. Dobado, D. Espriu and M. J. Herrero, *Chiral Lagrangians as a tool to probe the symmetry breaking sector of the SM at LEP*, *Phys. Lett. B* **255** (1991) 405–414.
- [87] M. J. Herrero and E. Ruiz Morales, *The Electroweak chiral Lagrangian for the Standard Model with a heavy Higgs*, *Nucl. Phys. B* **418** (1994) 431–455, [[hep-ph/9308276](#)].
- [88] S. Weinberg, *Phenomenological Lagrangians*, *Physica A* **96** (1979) 327–340.
- [89] G. Buchalla, O. Cata and C. Krause, *A Systematic Approach to the SILH Lagrangian*, *Nucl. Phys. B* **894** (2015) 602–620, [[1412.6356](#)].
- [90] G. F. Giudice, C. Grojean, A. Pomarol and R. Rattazzi, *The Strongly-Interacting Light Higgs*, *JHEP* **06** (2007) 045, [[hep-ph/0703164](#)].
- [91] V. Sanz and J. Setford, *Composite Higgs models after Run2*, [1703.10190](#).
- [92] G. Panico and A. Wulzer, *The Composite Nambu-Goldstone Higgs*, *Lect. Notes Phys.* **913** (2016) pp.1–316, [[1506.01961](#)].
- [93] G. Buchalla, O. Cata, A. Celis and C. Krause, *Comment on "Analysis of General Power Counting Rules in Effective Field Theory"*, [1603.03062](#).
- [94] A. Azatov, R. Contino, G. Panico and M. Son, *Effective field theory analysis of double Higgs boson production via gluon fusion*, *Phys. Rev. D* **92** (2015) 035001, [[1502.00539](#)].

- [95] M. Laine and A. Vuorinen, *Basics of Thermal Field Theory*, *Lect. Notes Phys.* **925** (2016) pp.1–281, [[1701.01554](#)].
- [96] D. J. H. Chung, A. J. Long and L.-T. Wang, *125 GeV Higgs boson and electroweak phase transition model classes*, *Phys. Rev.* **D87** (2013) 023509, [[1209.1819](#)].
- [97] C. L. Wainwright, *CosmoTransitions: Computing Cosmological Phase Transition Temperatures and Bubble Profiles with Multiple Fields*, *Comput. Phys. Commun.* **183** (2012) 2006–2013, [[1109.4189](#)].
- [98] M. Chala, G. Nardini and I. Sobolev, *Unified explanation for dark matter and electroweak baryogenesis with direct detection and gravitational wave signatures*, *Phys. Rev.* **D94** (2016) 055006, [[1605.08663](#)].
- [99] S. J. Huber and M. Sopena, *An efficient approach to electroweak bubble velocities*, [1302.1044](#).
- [100] T. Konstandin, G. Nardini and I. Rues, *From Boltzmann equations to steady wall velocities*, *JCAP* **1409** (2014) 028, [[1407.3132](#)].
- [101] L. Leita and A. Megevand, *Hydrodynamics of phase transition fronts and the speed of sound in the plasma*, *Nucl. Phys.* **B891** (2015) 159–199, [[1410.3875](#)].
- [102] D. Bodeker and G. D. Moore, *Can electroweak bubble walls run away?*, *JCAP* **0905** (2009) 009, [[0903.4099](#)].
- [103] D. Bodeker and G. D. Moore, *Electroweak Bubble Wall Speed Limit*, *JCAP* **1705** (2017) 025, [[1703.08215](#)].
- [104] C. Caprini et al., *Science with the space-based interferometer eLISA. II: Gravitational waves from cosmological phase transitions*, *JCAP* **1604** (2016) 001, [[1512.06239](#)].
- [105] H. Audley et al., *Laser Interferometer Space Antenna*, [1702.00786](#).
- [106] TLEP DESIGN STUDY WORKING GROUP collaboration, M. Bicer et al., *First Look at the Physics Case of TLEP*, *JHEP* **01** (2014) 164, [[1308.6176](#)].
- [107] G. Buchalla, O. Cata, A. Celis and C. Krause, *Standard Model Extended by a Heavy Singlet: Linear vs. Nonlinear EFT*, *Nucl. Phys.* **B917** (2017) 209–233, [[1608.03564](#)].
- [108] G. Buchalla, O. Cata, A. Celis and C. Krause, *Note on Anomalous Higgs-Boson Couplings in Effective Field Theory*, *Phys. Lett.* **B750** (2015) 298–301, [[1504.01707](#)].
- [109] C. P. Burgess, H. M. Lee and M. Trott, *Comment on Higgs Inflation and Naturalness*, *JHEP* **07** (2010) 007, [[1002.2730](#)].
- [110] G. Passarino and M. Trott, *The Standard Model Effective Field Theory and Next to Leading Order*, [1610.08356](#).
- [111] R. Grober, M. Muhlleitner, M. Spira and J. Streicher, *NLO QCD Corrections to Higgs Pair Production including Dimension-6 Operators*, *JHEP* **09** (2015) 092, [[1504.06577](#)].